An Investigation on Electrical Properties of Major Constituents of Grape Must Under Fermentation Using Electrical Impedance Spectroscopy

A thesis submitted in fulfillment of the requirements for the degree of Master of Engineering

Sicong Zheng

B.Eng

School of Electrical and Computer Engineering

Science, Engineering and Health College

RMIT University

August 2009

Declaration

I certify that except where due acknowledgement has been made, the work is that of the author alone; the work has not been submitted previously, in whole or in part, to qualify for any other academic award; the content of the thesis is the result of work which has been carried out since the official commencement date of the approved research program; and, any editorial work, paid or unpaid, carried out by a third party is acknowledged.

_____

Sicong Zheng

August 2009

Abstract

Electrical Impedance Spectroscopy (*EIS*) has been used for investigating structures of organic and inorganic materials since the 1960s. Recently, research on detecting physical and chemical changes in plants and biological tissues by *EIS* measurements has become a focus of interest. This research confirmed that *EIS* is effective in monitoring the ripening stages and physical damage to fruit, such as chilling and bruising. However, the *EIS* applications on wine fermentation analysis are rarely researched. Due to the huge rise of wine consumption all over the world, analytical tools on wine fermentation monitoring, which can measure major components in fermenting grape juice quickly, is required. As a rapid, inexpensive and simple method, *EIS* has great potential to replace the current slow response tools, such as High Performance Liquid Chromatography (*HPLC*) and Gas Chromatography (*GC*).

In this research, an investigation into the application of electrical impedance measurements to simulated solutions and grape musts is carried out. The dissertation outlines the experimental research conducted on relationships between impedance properties and concentration of major components of grape must. *EIS* measurements for monitoring ethanol, sugar, tartaric acid and malic acid changes in the process of fermentation are investigated. Experiments were performed on single solvent solutions, compound solutions and grape juice under fermentation.

As a result, linear relationships between impedance properties (including impedance magnitude on specific frequency, diameter of Nyquist plot and value of components in equivalent electrical circuits) and concentration of ethanol in pure solutions are found. Two major organic acids in grape juice, tartaric acid and malic acid, are also tested. Power relationships between malic and tartaric acid concentrations and solution resistance which is measured by *EIS* are found. It has also been discovered that the ionization resistance of organic acids has a linear relationship with the concentration of ethanol. Based on these findings, the ethanol concentration and organic acid concentrations in compound solutions can

be measured by *EIS*. Two models containing constant phase elements are established for high and low conductivity solutions and they fit the data better than any previous models, such as the Cole model and the Hayden model, etc. Validation experiments on ethanol solutions and real fermenting grape juice are also carried out to confirm the applicability of ethanol measurement in real condition.

In conclusion, this research proves that the impedance measurements are suitable to measure ethanol concentrations in fermenting grape must. They are rapid in response and easy to operate. This method may cause a revolution in current fermentation analysis. Further research may consummate the *EIS* method for industrial wine applications, and spread this method to applications in other alcoholic beverages and food products.

Table of Contents

List of Figures

List of Tables

Acknowledgements

I would like to express my special thanks to my supervisors, Dr. John Q. Fang and Prof. Irena Cosic for their support, suggestions and constructive criticism given throughout this research.

I'm grateful to the technical staff from Department of Food Sciences, RMIT University, Australia, for their technical assistance.

I would like to address my gratitude to Terry Flora, the manager of Mount Moliagul Winery, for his support with wine samples and many valuable suggestions.

I would also express my thanks to my friends, especially Miss Xing Liu, who have provided many valuable suggestions.

I wish to express my sincere gratitude to my parents and my uncle's family who have supported me and guided me during my candidate period.

Chapter 1
Introduction

1.1 Overview

This chapter outlines the motivation for conducting this research, the research problems faced in studying impedance properties of wine, objectives, and their contribution to this thesis. In this chapter, the background of winemaking and current wine analytical techniques are elucidated. Research problems faced in studying impedance properties of wine and relevant conclusions are stated within this chapter.

1.2 Background and Motivation

Wine means the product arising from the complete or partial fermentation of fresh grapes or products derived solely from fresh grapes [1].

Grapes are one of the most popular fruit for both table eating and winemaking. The total yield of grapes harvested in 2007 in Australia was 1,530,439 tonnes. Among them, 1,370,690 tonnes (close to 90%) were used for winemaking [2]. Wine grapes are mostly grown between thirty and fifty degrees north or south of the equator. Countries in this area produce more than 23,000,000 tonnes of wine each year [3]. The wine trading market provides huge economic profits for these winemaking countries every year. As one of the biggest wine exporting countries, Australia has high quality wine production which occupies a remarkable place in the world wine market. However, the quantity of wine exported from Australia is still half that of the European countries. Therefore, the quality of wine is more important than quantity in Australia. It is clear that consumers all over the world are expecting higher quality wines. Due to this expectation, improvement in wine quality control is very necessary.

Grape wine was originally used in European countries as a special alcoholic beverage in religious ceremonies and other important occasions. Now grape wines, which contain rich flavours with abundant varieties, are popular all over the world, including East Asia and Africa. It is also recognized that wine contains a variety of antioxidants which provide protection for the human circulatory system. Since wine became an industrial product instead of a home-made beverage, research on wine science has benefitted wine making a lot. Through research in wine science, winemakers can better understand grape growing, the biochemistry and microbiology of wine fermentation, flavour adjustment and the changing of various components during aging.

Wine analytical techniques have become essential tools of modern winemaking. Winemakers rely on chemical and physical analytical techniques to understand their product precisely. These analytical tools not only measure content of chemical components in grapes, grape juice and fermented wine, such as sugar,

organic acids, ethanol, etc; but also establish a standard of quality in wine products which are accepted by consumers.

Traditionally, winemakers measured the quality of wine by human sense, including vision, olfaction and gustation. Since modern science developed, chemical and physical analytical tools are used for quality determination and production control. These tools include: refractometers for sugar content measurement; High Performance Liquid Chromatography (*HPLC*) for ethanol measurement; carbohydrates and organic acids measurement; Atomic Absorption Analysis (*AA*) for metal component measurements; Titrametric for titratable acidity and sulphur dioxide measurements; and spectrometry for pigment and tannin measurement; etc. Obviously, the major disadvantage of the traditional chemical and physical tools for wine analysis can now be seen. By these measurements, results come slowly and were more complex. In some traditional measurements, expensive equipment is also require

d. That means an online control system for wine production is hard to develop and popularize with such traditional tools.

Recently, many new methods of wine component measurement are under development. Ultrasound based measurements [4] have been developed for ethanol and sugar content determination during fermentation and aging. Shortwave-near infrared spectroscopy and microwave based measurements [5] are under research as well for ethanol determination in wine products. As can be seen, most of these researchers are trying to find a method which can measure important wine components quickly and easily. Such equipment is expected to have the following features: quick response, easy to operate, low cost and portability.

Impedance measurement has been used as a tool for food quality assessment for several years. Electrical Impedance Spectroscopy has been widely used to investigate the fundamental electrical properties of plant tissues and to detect tissue changes under different physiological conditions since the beginning of the 1990s [6]. Sensitivity assessment of damage caused by bruising or chilling on fruit and plants has been confirmed by using impedance measurements [7, 8].

Previously, researches on electrical impedance spectroscopy applied in ion detection in solutions were also carried out [9]. In biomedical fields, electrical impedance measurements for DNA detection [10], human mesenchymal stem cell growth [11], antibodies detection [12], were researched recently. Obviously, Electrical Impedance Spectroscopy (*EIS*) is showing that it has a great future in food quality assessment. Since research reports are found rarely in application of the *EIS* method on wine quality control, this research project investigates the possibility for application of electrical impedance spectroscopy on wine making process control. This thesis proposes the measurement of important components in grape juice during wine fermentation by EIS method. The achievement of this rapid wine fermentation monitoring method will lead to better quality control of winemaking.

1.3 Objective of Research

The objective of this research is to investigate the electrical impedance, resistance, reactance and other properties of fermenting grape juice, and to propose new methods for measurement of the fermentation parameters.

Firstly, a better understanding of the electrical impedance properties of organic compounds in aqueous solutions has to be provided. There is the ionization balance and the mass balance of soluble organic compounds in solutions. In complex solutions (e.g. wine), the analysis of electrical impedance spectroscopy may lead to a new method for detecting the concentrations of specific solutes efficiently.

Secondly, this research will improve existing models of impedance properties of plant materials. Constant Phase Element (*CPE*), which was proposed by Cole [15] and improved by many other researchers, such as Zoltowski [56] and Lasia [55], has been used widely for electrical impedance spectroscopy models. This thesis examines whether *CPE* theory and other existing models are suitable to analyse electrical impedance properties of complex solutions.

Thirdly, this research will establish a rapid response method for fermentation monitoring by using electrical impedance spectroscopy analysis for closed loop automated systems in wine fermentation management.

1.4 Contributions

This research covers the electrical properties analysis of ethanol, organic acids, sugar, compound solutions and real fermenting grape juice. By carrying out experiments with these different types of samples, this research has achieved the following contributions:

The effective frequency range for electrical impedance spectroscopy for ethanol and sugar solutions has been determined to be from 100*Hz* to 1*MHz*, due to the polarization under low frequencies in dielectric solutions. The effective frequency range for measuring concentration of organic acid solutions has been from 1*Hz* to 100*Hz*, which is easier to analyze.

By analysis of Nyquist plot of ethanol aqueous solutions, a linear relationship between concentrations of ethanol and the diameter of its Nyquist plot is found. This linear relationship has been proven to measure ethanol concentrations efficiently.

In ethanol solutions, impedance magnitude values and reactance of specific frequency can indicate the concentration. That means, single frequency impedance can also be applied in ethanol concentration measurement.

An equivalent electrical model which consists of a resistor parallel with a Constant Phase Element (*CPE*) is developed and tested for ethanol pure solutions and sugar-ethanol compound solutions. The resistor value and two parameters of CPE (*CPE-T* and *CPE-P*, please see details on section 3.3.1.3, page 49) are analyzed. The value of resistor components in the model shows good correlation with the concentration of ethanol in an aqueous solution. However, *CPE-T* value is constant and independent to different concentration of solutions. *CPE-P* value is also not suitable to indicate the concentration of ethanol due to its poor correlation, though it can be described well theoretically.

By testing the simulated wine solutions which contain sugar and ethanol, it has been found that the electrical impedance spectrum can be used to indicate the end of fermentation. A remarkable rise in the diameter of Nyquist semi-circle occurred when the sugar concentration fell close to zero.

In pure and compound solutions of malic acid and tartaric acid, a model consist of a resistor (*Rs*) serial with a *CPE* is established and tested. A power correlation between the values of Rs in the simulated electrical circuits and acid concentration is found. This finding provides the possibility to measure the malic acid concentration by *EIS*.

A simulated solution with malic acid, tartaric acid and ethanol in concentration of real fermentation condition is analysed. A linear relationship between ethanol concentration and *Rs* value is discovered. It is confirmed that the variation of malic acid concentration can hardly influence the impedance measurement of ethanol concentration.

1.5 Thesis Organization

The experimental protocol of this research is followed in this order: 1, *EIS* on pure solutions; 2, *EIS* on compound solutions; 3, Validation on real fermentation. Based on the experimental protocol, and in order to present the background, the methodology and the harvest, this thesis is divided into six main chapters:

Chapter 1 forms an introduction of this research, including motivation, objective and contributions.

Chapter 2 provides background knowledge of winemaking procedures, wine analysis techniques and electrical impedance analysis. It includes knowledge about wine components, wine analysis techniques which are currently used, basic knowledge of electrical impedance, measurement methods and data analysis methods.

Chapter 3 investigates electrical impedance spectroscopy of ethanol solutions, tartaric acid solutions and malic acid solutions. Different data analysis methods are applied to analysis of the electrical impedance spectrum of ethanol solutions. The results of impedance measurement in pure organic acid solutions are also analysed.

Chapter 4 investigates impedance properties of compound solutions. Samples include mixture of tartaric acid and malic acid. A series of simulated solutions contain ethanol, tartaric acid and malic acid with concentrations of real condition are also researched.

Chapter 5 validates the *EIS* methods established above for ethanol concentration measurement in simulated solutions and real fermenting grape juice. A discussion for application of *EIS* method in wine industry is carried out.

Chapter 6 concludes the overall study with several recommendations for future research.

Chapter 2
Literature Review

2.1 Overview

This chapter provides the background knowledge in bio-impedance study, general knowledge of winemaking, wine analytical tools and recent researches on plant and food assessment. Basic knowledge about passive electrical circuits and their impedance is provided. Current analytical tools of wine analysis and related knowledge are also explained. Recent research for Electrical Impedance Spectroscopy and related equivalent electrical circuit models on its practical applications are elaborated. Data analysis methods and statistic tools used in this research are also provided. Applications which are based on recent impedance studies on plant and food assessment are provided.

2.2 Basic Theory of Electrical Impedance

In order to understand the essence of impedance, elements in passive electrical circuits should be described. Passive circuit elements are components that do not generate current or potential in a passive electrical circuit, which contain only passive circuit elements. There are three passive circuit elements, including Resistors, Capacitors and Inductors.

The relationships between current and potential for Resistor (*R*), Capacitor (*C*) and Inductor (*L*) are:

Resistor: $$V(t) = RI(t) \tag{2-1}$$

Capacitor: $$I(t) = C\frac{dV(t)}{dt} \tag{2-2}$$

Inductor: $$V(t) = L\frac{dI(t)}{dt} \tag{2-3}$$

Where *R*, *C*, *L* are values of resistance, capacitance and inductance. As can be seen, if *dV/dt* is zero, which means the potential is steady, the *I(t)* is zero according to the definition of capacitor, which means the capacitor is equivalent to an open circuit. In the same way, if the current is steady, an inductor is equivalent to a short circuit according to the definition of inductor.

When a sinusoidal potential is applied on a passive circuit:

$$V(t) = |\Delta V|\cos(\omega t) \tag{2-4}$$

The current response is:

$$I(t) = |\Delta I|\cos(\omega t + \varphi) \tag{2-5}$$

Where ω is the radian or angular frequency of applied signal.

According to equation 2-2, if a single capacitor is set in the circuit, the current response of the capacitor is:

$$\Delta I = jC\omega\Delta V \tag{2-6}$$

Where j is the imaginary number. This expression shows that the current is out of phase with the potential difference.

Similarly, for an inductor, the potential response is:

$$\Delta V = j\omega L\Delta I \tag{2-7}$$

which shows that the potential difference is out of phase with the current.

And for a pure resistor, Equation 2-1 can be written as:

$$\Delta V = R\Delta I \tag{2-8}$$

It can be concluded that, the impedance Z, which is defined as "the ratio of the phasor voltage V to the phasor current I" [16]:

$$Z = \frac{\Delta V}{\Delta I} \tag{2-9}$$

Impedance is a combination of all the value passive circuit elements in that circuit. It is a frequency-dependent quantity and measured in Ω.

Since impedance is a complex quantity, it can be described as having real and imaginary components:

$$Z = R + jX \tag{2-10}$$

where R is the real component (resistance), and X is the imaginary component (reactance). The reactance may be positive or negative. The impedance is shown graphically on a phasor diagram (Figure 2-1).

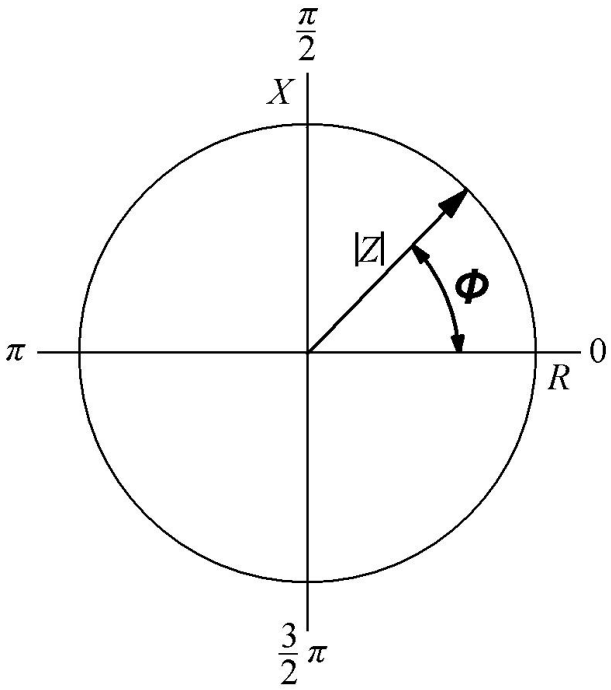

Figure 2-1 Impedance Phasor Diagram, which shows the relationships between complex impedance magnitude and phase angle

The impedance can also be expressed in polar form as:

$$Z = |Z| \angle \phi \tag{2-11}$$

where

$$|Z| = \sqrt{R^2 + X^2} \tag{2-12}$$

$$\phi = \tan^{-1} \frac{X}{R} \tag{2-13}$$

and

$$R = |Z| \cos \phi \tag{2-14}$$

$$X = |Z| \sin \phi \tag{2-15}$$

Based on the above illustrations, the equivalent impedance of resistors, inductors, and capacitors in passive electrical circuits can be obtained from the following equations:

For a pure resistor,

$$Zr = R \tag{2-16}$$

For a capacitor,

$$Zc = \frac{1}{j\omega C} \tag{2-17}$$

And for an inductor,

$$Zi = j\omega L \tag{2-18}$$

These impedance responses are used to construct the response of whole circuits.

2.3 Basic Knowledge of Wine Analysis

2.3.1 Chemical components of Grapes and Wine

The main grape berry components in roughly decreasing order by concentration are water and other inorganic substances, carbohydrates, acids, phenols of all types, nitrogen compounds, terpenoids, fats and lipoids, volatile odorants, or other flavoring compounds. A typical amount of these components expressed by percentages of weight are given in Table 2-1.

Table 2-1 Rough estimate of the typical percentages by weight of components of wine grapes at harvest, in berries and juice, compared with that of dry table wines. [13]

			Dry Table Wines	
Class of compound	Berries	Juice	From juice	Pomace fermented
Water	74	76	86	85
Inorganic salts	0.5	0.4	0.2	0.2
Carbohydrates	24	23	3	4
Alcohols	0	0	10	10
Acids	0.6	0.7	0.7	0.6
Phenols	0.2	0.01	0.01	0.1
Nitrogenous compound	0.2	0.1	0.1	0.05
Lipids	0.2	0.01	0.01	0.02
Terpenoids	0.02	0.01	0.01	0.015
Other volatiles	0.01	0.01	0.1	0.1
Miscellaneous	0.1	0.01	0.5	0.1
Total	100	100	100	100

2.3.1.1 Water and Minerals in Grape Berries

As a typical fruit, grape berries contain approximately 75% water. Grape plants also require a variety of minerals including potassium, magnesium and calcium. Most of these are inorganic anions of nitrate and phosphate. Sulfur, iron and other trace minerals are also needed in varying amounts by grape plants. The total minerals (ash content) of ripe grape juice is from 2 to 6 *g/kg*. [13]

2.3.1.2 Sugar Species in Grape Juice

Glucose and fructose are both six-carbon sugars, which are the most common sugars in grapes. They occur in approximately equal concentrations in grapes, making up a very high percentage of the total soluble carbohydrates. As a result, sucrose, which is hydrolysed to glucose and fructose, is low in grapes. However, *Brix* (by definition gram of sucrose per 100g solution) is still generally considered as a sugar concentration measure in most cases. The Brix range of grape musts are normally from 20 to 25. [13]

2.3.1.3 Ethanol and Its Effect in Wines

Ethanol is obviously the most important component in wine. It is a volatile, flammable and colourless liquid which can be found in all alcoholic beverages. It not only builds the body of a wine, but also affects its flavour and estimates its species. The ethanol in wine is mainly produced by yeast fermentation. The whole transformation of grape must into wine can be described as: wine yeast (such as *Saccharomyces*) metabolizes glucose and fructose to pyruvate via the glycolytic pathway, and then primarily in order to recycle cofactors, pyruvate is decarboxylated to acetaldehyde, which is then reduced to ethanol. [13]

The production of ethanol is highly related to many factors in the fermentation period. These factors can be defined as the ability of yeast production and environment factors. Species and strains of yeast vary in ability to convert carbohydrates to alcohol and other byproducts. When the fermentation is finished, there could be two situations. One is the alcohol content which is close to the upper limit for yeast to survive. Though sugar in grape must still exist, the growth of yeast tends to stop. The other situation occurs when the sugar in grape must has been totally consumed.

As a major part of alcohol compounds in wine, ethanol content is also defined as a principal basis of wine taxation. In the United States, a regular definition of wine is a beverage which contains alcohol between 7 and 24% (*v/v*). In the U.S federal definition, “table wines” must contain between 7 and 14% (*v/v*), and “dessert wines” between 14 and 24% (*v/v*). [17] In Australia, wine and sparkling wine

must contain no less than 80 *ml/L* of ethanol at 20 °*C* [1]. Due to this situation, the alcohol and ethanol content is transparently the most significant for wine indexing.

2.3.1.4 Major Acids and Their Effect in Grape Juice and Wine

As well as the two major acids, tartaric acid and malic acid, small amounts of citric, isocitric, aconitic, glutaric, fumaric, pyrrolidone carboxylic, 2-ketoglutaric, and shikimic acids may also be found in grapes and their products. These free acids keep the grape juice to a low pH, which is not only the cause of sourness, but also helps to control the microbiological environment for yeast and chemical reaction in wine production. Tartaric acid (H_2T) and its salts are important to the stability of wine. Its content in grape must ranges from 2.0 to 10*g/L* and varies according to region, variety, maturity, soil and viticultural practices. [17] Tartaric acid is formed as ionized bitartrate and tartrate in grapes. In grape must and wine, tartaric acid is formed as H_2T, HT^- and T^{2-} ions, which all exist in the juice. The acid dissociation constant of H_2T and its ions are described in 2-12.

$$H_2T \xleftrightarrow{pKa = 2.98} HT^- \xleftrightarrow{pKa = 4.34} T^{2-} \tag{2-12}$$

Malic acid is another important acid in grapes and wine. In malolactic fermentation, malic acid is converted to lactic acid by malolactic conversion carried out by the malolactic bacteria.

2.3.1.5 Phenols Components in Grapes and Wine Products

The phenolic substance is quite important for wine characteristics and quality, as it includes red pigments, brown-forming substrates, the astringent flavours and the bitter substances in grapes and wines. They affect the colour of red wine, astringency and bitterness. All of these phenolic compounds are derived from the structure of hydroxybenzene. Phenols in grapes can be divided into two classes, which are nonflavonoid phenols and flavonoid phenols. Most of the phenols in grape juice are nonflavonoid phenols, and their concentrations are not high enough to present a flavour. The level of those nonflavonoid phenols is relatively constant in grapes [17]. Flavonoid phenols are found in the skins, seeds and pulp of grape berries. They impact on the structure and colour of wine. In grape juice and wine, complex phenols are called tannins, which are polymers of both

flavonoid and nonflavonoid phenols. This blue-colour complex which can react with protein is described as an astringent.

2.3.1.6 Nitrogenous Substances and Other Components

The major nitrogen-containing components in grapes are ammonium salts, amino acids and peptides, proteins and nucleic acid derivatives. The total nitrogen content of grape must ranges from 60 to 2400 *mg(N)/L*. [17] They play an important role in fermentation and clarity. For example, peptides are ingested by lactic acid bacteria during the malolactic fermentation, which is the secondary fermentation carried out by these bacteria [16]. On the other hand, the soluble proteins in grapes cause amorphous haze in bottled wines.

Lipids, terpenoids, volatile aroma compounds and miscellaneous compounds also influence the flavour of wine. The amount of these components is not enough to affect fermentation. As a result, they are normally not controlled by winemakers.

2.3.2 Current Wine Analysis Technologies

As mentioned before, the components of wine can be divided into different classes, which are analysed during the production process. Table 2 shows common analysed components of wine. Analysis of grapes and wines can improve the quality control of wine production; reduce the spoilage during the production, lead to more precise blends of wines, and provide evidence to meet requirements of trade laws and certification.

Table 2-2 Common components analysed in Wine [17]

Soluble solids: *"Sugar," extract, glucose, and fructose*
Acidity: *total, volatile, pH, individual acids*
Alcohol: *ethanol, methanol, fusel oils, glycerol*
Carbonyl components: *acetaldehyde, HMF, diacetyl*
Esters: *ethyl acetrate, methyl anthranilate (labruscana)*
Nitrogen components: *ammonia, amino acids, amines, proteins*
Phenolic components: *total, phenolic fractions including anthocyanins*
Chemical additions: *sulphur dioxide, sorbic and benzoic acids, illegals*
Other: *common and trace metals, oxygen, carbon dioxide, fluoride*

Current analytical techniques used in wineries and service laboratories include chemical techniques, High Performance Liquid Chromatography (*HPLC*), Atomic Absorption (*AAS*), Gas Chromatography (*GC*), Gas Chromatography / mass spectrometry (*GC-MS*), and Near Infrared Spectroscopy (*NIS*). New methods, which are still under research, such as ultrasound measurements and microwave measurements are hardly applied in industrial production.

2.3.2.1 Chemical Techniques Used in Wine Analysis

Chemical techniques are the basis of other analytical techniques. Most other techniques also require pretreated samples by chemical reaction. Some important wine quality indices, such as total acidity, carbohydrates, ethanol, reducing sugar, total nitrogen and total phenols can be tested by titrametric. As a primary chemical technique, titrametric is usually low cost. However, they can only be operated by trained testers. Furthermore, long preparation time and low precision of visual readings limit its application.

2.3.2.2 High Performance Liquid Chromatography

High Performance Liquid Chromatography (*HPLC*) is a form of column chromatography used widely in biochemistry and analytical chemistry fields since its development in the 1970s. It consists of a column which holds chromatographic packing material (also called stationary phase), a pump that moves the mobile phases through the column, and a detector which shows the retention time of molecules. As the retention time changes with the interaction among the molecules, the stationary phase, and the mobile phases, the mixed molecules can be separated, identified, and quantified. [18] In the wine industry, *HPLC* is applicable to test most organic acids, sugars, phenolics and also alcohols. It can present the result rapidly and precisely with small amounts of samples, however this method still needs professionals to operate the machines and the cost of equipment is obviously high.

2.3.2.3 Atomic Absorption Spectroscopy

Atomic Absorption Spectroscopy is used to determine the concentration of a particular metal element in the wine sample. It was developed in the mid 1950s.

Since then there has been an extremely rapid growth in the use of this technique. [19] When atoms absorb a fixed quantity of energy, or light with a specific wavelength, electrons of these atoms can be promoted to higher orbital. The quantity of energy or wavelength of the applied light is specific to a particular electron transition in a particular element. As the quantity of energy absorbed by the sample can be measured, the concentration of the target element can be calculated.

2.3.2.4 Gas Chromatography

Theoretically, Gas chromatography (*GC*) can be used for determination of a variety of food components including fatty acids, triglycerides, cholesterol and other sterols, alcohol, and simple sugars, as well as oligosaccharides, amino acids and peptides, vitamins, pesticides, herbicides, food additives, antioxidants, flavour components, etc. [20] In the wine industry, *GC* is normally used for alcohol and ester testing. The hardware of a *GC* system includes: gas supply system, injection port, oven, column and stationary phases, and detectors. Like *HPLC*, *GC* is also based on the same theory: The stationary phase is chosen to permit differential interaction with the components of the sample to be resolved. [20] To quantify ethanol, a series of standards of known concentration should be prepared. Comparing with the *GC* response between those samples, the concentration of unknown samples can be found out.

2.3.2.5 Gas Chromatography – Mass Spectrometry

Gas Chromatography – Mass Spectrometry (*GC-MS*) is the combination of gas chromatography for separation and mass spectrometry for detection and identification of the components of a mixture of compounds. Practically, *GC* has a few weaknesses such as its requirement for volatile compounds, identification of compounds by retention time by most detectors. It lacks definitive proof of the nature of the detected compounds as they are separated. The mass spectrometer takes injected material, ionized in a high vacuum, propels and focuses these ions and their fragmentation products through a magnetic mass analyser, and then collects and measures the amounts of each selected ion in a detector. [21]

Therefore, *GC-MS* can measure non-volatile compounds or trace amount compounds such as sulphides, ethyl carbamate, and phenols.

2.3.2.6 Near-infrared Spectroscopy

Near-infrared spectroscopy (*NIS*) is a spectroscopic method which uses the near infrared region of the electromagnetic spectrum to measure compounds. It has taken its place among other proven spectroscopic tools, especially for determining chemical and physical properties of foods and food products. [22] Constituents/properties in foods determined with *NIS*, which is sensitive to the *CH*, *NH* and *OH* absorption in food components, include water, protein, fats, dietary fibre, sucrose, carbohydrates and saccharin, etc.

2.3.2.7 Ultrasound and Microwave Based Measurement

Recently, new methods for wine analysis are under investigation by researchers. Ultrasound has been reported as a potential tool in measuring sugar and ethanol concentrations in hydroalcoholic solutions [4]. The speed of ultrasound transmitted through solutions is highly related to the density of solutions. However, the ultrasound transmission pathway is easily blocked by containers like the fermentation tank. Also carbon dioxide bubbles, which influence the ultrasound speed a lot, limit the development of this method. Microwave is applied to the determination of alcohol and sugar content in water as well. Meriakri and Chigrai [5] reported microwaves of 2.3 *GHz* and 9 *GHz* can be efficiently used to measure the concentration of alcohol and sugar in solutions.

2.4 Electrical Impedance Spectroscopy

Electrical impedance experiments use a signal generator to input a potential signal of steady or variable frequency. The input signal and the resulting signal is processed and produces a frequency-dependent transfer function, which is impedance. This section will show the researches which have been carried out on bio-applications.

2.4.1 Single and Multiple Frequency Impedance Measurement

As its name implies, single frequency measurement uses sine or cosine waves to measure the complex impedance responding to the single frequency input signal. It usually uses 50 kHz as the working frequency to estimate total body water and the fat free mass of the human body [23]. The choice of 50*KHz* is because it is in the frequency range where extracellular fluid contributes to conduction and intracellular fluid starts to contribute [24]. Surface electrodes are placed on hand and foot [25, 26]. Cell membrane which acts as an insulator at low frequency separates cell into intracellular space and extracellular space [27].

Although single frequency measurement can be efficient in the measurement of the human body, it is limited when the distribution between extracellular and intracellular fluids is to be observed, such as in cirrhosis [28-30]. It is suggested that multiple frequency measurement can improve prediction of body composition. Such a technique is frequency sweeping [30]. The prediction of extracellular water is measured by low frequency impedance measurement (i.e. 1-5 *kHz*) [30, 31]. Whilst, high frequency impedance measurements (i.e. 100-500 kHz) are also used in total water measurement [30, 31]. Reactance against resistance is plotted in a complex plane, the frequency at the peak of the plot is the so-called characteristic frequency. Current flows through both extracellular water and intracellular water at the characteristic frequency. Impedance measured at the characteristic frequency is related to the estimation of total water. Frequencies of 1, 5, 50,100, 200 to 500 kHz are generally employed in several evaluations [27, 32].

2.4.2 Electrical Impedance Spectroscopy

Electrical impedance spectroscopy (*EIS*) is used for studying the structures of organic and inorganic materials with wide and continuous frequency impedance measurement [33]. It deals with complex quantities. It analyses the subsequent electrical response of a subject when small *AC* signals are applied and characterizes the physicochemical properties of the system [34]. The span of frequencies used in *EIS* ranges from about 10^{-5} *Hz* to about 10^{7} *Hz* [35]. *EIS* generally makes use of equivalent circuits to characterize experimental frequency response.

Once there are suitable mathematical models available for the specific physicochemical process, they should be used to fit the data from the *EIS* experiments. Otherwise, built up equivalent electrical circuits could be used to analyze the various changes that take place during the physical process of the particular system. The major applications of *EIS* are in the investigations of fuel cells, rechargeable batteries, and corrosion [34]. It has also been used in the biological area, such as the studies of human body fluid as well as animal and plant tissues [7, 27, 36, 37] etc.

2.4.3 Electrodes Configuration and Connection Methods

The most commonly employed approach in biological tissue investigations is the two-electrode configuration. The impedance output includes the impedance response associated with the working electrode interface, the counterelectrode interface, and the electrolyte between the working and the counterelectrodes. The measured impedance contains the electrode polarization impedance. When polarisable electrodes (steel, copper) are used, the electrode and tissue contact impedance has to be considered. The electrode polarization impedance is caused by the electrochemical reaction which occurs in the contact interface between electrodes and tissue when polarisable needle electrodes impale plant tissue. It has been postulated that the impedance of an electrode-electrolyte interface depends on electrode material, electrolyte concentration, and temperature [38]. Harker et al. [39] reported that electrode polarization impedance can be very large and many times larger than the sample impedance at low frequencies, which can lead to

inaccuracies in the measurement. Electrode polarization impedance is mainly apparent at frequencies below 1 *kHz*, and is a severe problem below 20 Hz [40]. Therefore, it is important to eliminate the effect of electrode polarization impedance from tissue impedance while analyzing data.

Various methods have been proposed to reduce the effects of *AC* polarization impedance. Surface treatment of electrodes can be used to reduce the polarization impedance significantly, for instance, electrolytic deposition of colloidal platinum on platinum [40, 41]. The inter-electrode distances method has been widely used to correct electrode polarization impedance in several experiments [42, 43]. The principle of the inter-electrode distances method can be summarized as impedance measurements performed at three different inter-electrode distances at each frequency. The three sets of measured resistances and reactances against different inter-electrode spacing are plotted separately. The linear least squares regression is used to calculate the corresponding slope and intercept. As a result, the slope represents the value of resistance and reactance of tissue, whilst the intercept represents the value of resistance and reactance of the electrode. Consequently, the impedance of tissue sample and electrode are separated. Sufficiently high frequencies can reduce the electrode polarization impedance. Glerum [44] and Repo [45] introduced frequencies higher than 500 *Hz* to minimize the electrode polarization impedance. Freywald et al. [46] used a frequency spectrum starting at 4 *kHz* to reduce the electrode polarization impedance.

In contrast to the two-electrode configuration, the four-electrode configuration uses one pair of electrodes for voltage or current excitation, and another pair of electrodes for potential measurement. When the four-electrode measurement is employed, there is no current flow through the voltage measurement electrodes, thus there is no voltage drop across these electrodes, and the problem of electrode polarization can be largely eliminated.

Figure 2-2 shows the circuit sketch of 2-electrode, 3-electrode and 4-electrode measurements.

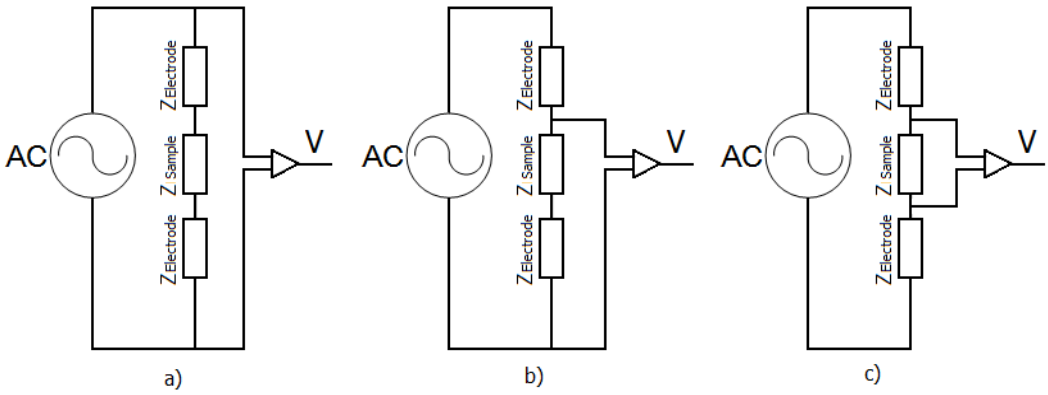

Figure 2-2 Circuit of different electrode configurations. a) 2-electrode configuration; b) 3-electrode configuration; c) 4-electrode configuration.

The two-electrode measurement is the most accurate at high frequencies, but the measurement is time consuming. In addition, the electrode polarization impedance affects the measurement very much especially at low frequencies, and the influences of electrode polarization impedance increase with frequency decrease. The four-electrode technique is a highly efficient method and largely minimizes the electrode polarization impedance problem. It can be useful when the sample is undergoing rapid changes within a short time, such as bruising and chilling. Therefore, the four-electrode configuration was carried out in these experiments.

2.4.4 Electrical Modeling of Plant Tissue and Electrolyte Solutions

In order to study the electrical properties of plants, the plant cell structure has been simulated by equivalent electrical circuits. The values of circuit components determine the electrical response. A single cell isolated from a tissue was simulated by an equivalent circuit consisting of resistors and capacitors arranged in series and parallel. Thus, a tissue block can be presumed to be a network of cells, which contain numerous arrays of mini-circuits [42, 48]. It is desirable that the equivalent circuit should include as few frequency-dependent elements as possible [48, 49]. There are several electrical models regarding the electrical properties of biological tissues that have been proposed by researchers, such as the *Cole* model, the *Hayden* model and the *Double-shell* model etc. Figure 2-3

displays a few popular simulated electrical circuits based on models for representing tissue blocks. All these models were constructed for the ideal case, which assumes that the tissue structure, dimension, shape, and orientation are uniform.

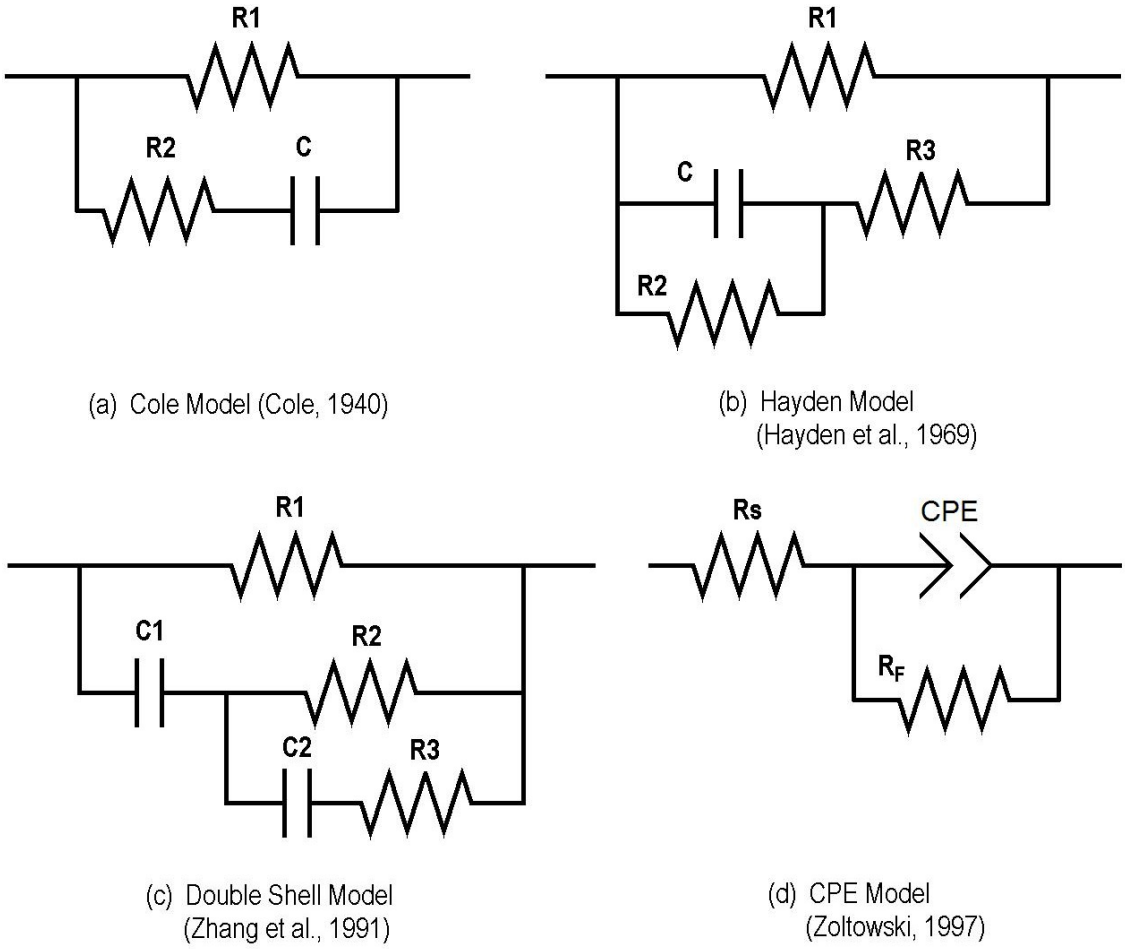

Figure 2-3 Electrical circuit models developed previously for electrical impedance simulation for plant tissue and electrolyte solutions

The *Cole* model, which is the simplest electrical model for a biological body, is shown in Figure 2-3 (a). The Cole model simplified biological tissue into a two-branch parallel circuit. *R1* represents the extracellular space resistance, *R2* represents the intracellular space resistance, and C represents the cell membrane capacitance. Tissue impedance at low frequencies is almost independent of cell membrane and internal resistivity [15, 50], which is due to the cell membrane

acting as a capacitor. The cell membrane is open-circuit at very low frequencies, while it is short-circuit at high frequencies.

Hayden model, which is presented in figure 2-3 (b), was proposed by Hayden and his co-workers [51] when they explored the quantitative relationships between plant impedance and temperature and humidity. The cells of potato tubers were examined under a microscope and they were found roughly isodiametric. Therefore, according to plant cell structure, the cells are equivalent to many small capacitor-resistors connected in parallel with their cell walls. In the simulated circuit, *R1* represents the resistance of all cell walls, *R2* represents the resistance of all membranes of all actual cells, *R3* represents the resistance of cytoplasm of actual cells, and *C* represents the capacitance of all membranes of actual cells.

Compared with the *Hayden* model, the *Double-shell* model adds one more branch, which is the resistance of vacuole and capacitance of tonoplast in series (Figure 2-3 (c)). The various components in the circuit include the cell wall resistance (*R1*), cytoplasm resistance (*R2*), vacuole resistance (*R3*), plasma membrane capacitance (*C1*), and tonoplast capacitance (*C2*). The double-shell model has been validated in several plant investigations, such as the impedance measurements conducted on nectarine fruit [52], persimmon fruit [8], kiwifruit [37], and leaves of *Peperomia obtusifolia* L. and *Brassica oleracea* L. [53].

Recently, the constant phase element (*CPE*) was introduced to improve the equivalent electrical circuit models which more closely fit real impedance spectra. CPE can be considered as a double layer capacitor on the electrodes. In fact, the CPE is equivalent to a distributed parameter circuit. [54] pointed out that in the case of a *2D* distribution, the local impedance spectrum does not contain a *CPE* element while in the case of a *3D* distribution, all the impedance spectra shown in a distributed network are identical and present *CPE* behaviour. When an alternative current was added to a solution such as ethanol, the solution itself can be considered as a transmission line, which has no individual components. As the phase angle of the transmission line is constant, the *CPE* was used to replace the distributed parameter circuit.

The impedance of *CPE* is calculated by equation below [55]:

$$Z_{CPE} = \frac{1}{T(j\omega)^{\phi}} \tag{2-19}$$

Where ω is frequency, T is a constant in *F cm-2 sΦ-1*, and Φ is a parameter usually between 1 (corresponding to a pure capacitance) and 0.5. In this paper, same as the *Z-View*® software, Φ is named as *CPE-P*, and T constant is named as *CPE-T*. Figure 2-3 (d) presented a simulated electrical circuit developed by Zoltowski [56] which contain a *CPE* element.

2.5 EIS Data Analysis

2.5.1 Data Representation

Once the raw data from experiments have been obtained, it is important to extract characteristic parameters to analyse the system properties. There are a few ways the data can be plotted, such as the Nyquist and Bode plane plotting. In this research, Nyquist plots are mainly used to analyse *EIS* data.

The Nyquist Plot is named after Harry Nyquist. It is also known as the complex plane, which generally plots the negative of the imaginary part of impedance against the real part of impedance. Impedance measurements were only conducted in the high frequency range initially where the electrode-electrolyte interface exhibits only a capacitive behavior. Thus, the imaginary part of impedance is negative. In order to plot data in the first quadrant, the sign convention has been adopted in the Nyquist Plot [57]. Figure 2-4 gives an example of the Nyquist Plane. In practice, there are no intercepts of real axis at relative low and high frequencies, owing to the existing equipment not being able to measure such frequencies. Therefore, the values of R_∞ and R_0 are calculated by extrapolation and interpolation respectively from the values obtained over frequency range [58].

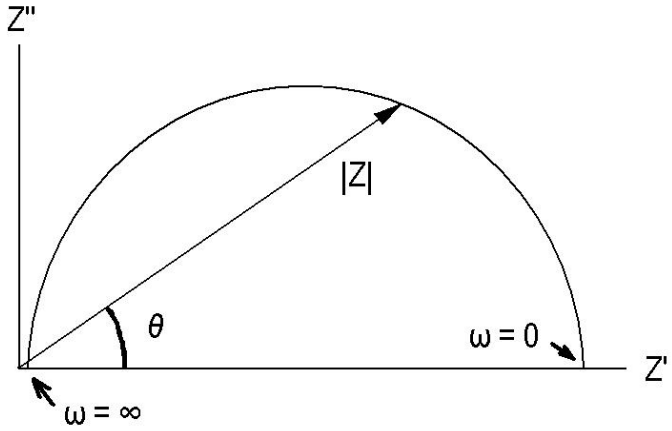

Figure 2-4. A typical Nyquist Plot. As shown, the Nyquist plot is resistance against reactance in Cartesian coordinates. The direction of frequency scan is 0Hz to ∞Hz.

2.5.2 Statistical tools

Common statistical tools are used to verify the veracity of results which are calculated or fitted from experimental data.

Standard deviation (σ) is one of the most widely used measures of dispersion. The formula [59] is:

$$\sigma = \sqrt{\frac{\sum_{i=1}^{n}(X_i - \overline{X})^2}{n-1}} \tag{2-19}$$

Coefficient of variation (Cv) is usually used to compare the dispersions of two distributions with markedly different means. It is calculated by equation 2-20:

$$Cv = 100 \times \left(\frac{\sigma}{\overline{X}}\right) \tag{2-20}$$

As seen in the equation, the larger the value of Cv, the larger is the dispersion relative to the mean. [59] On the other hand, it can avoid the influence of a data unit as Cv has no unit. In this research, Cv is used to display the errors of least square fittings in Nyquist semi-circle diameter analysis in ethanol solutions.

Coefficient of Determination (R^2) is a number between 0 and 1 which reveals how closely the estimated values for the fitted line correspond to the experimental data. The fitted formula is more reliable when the coefficient of determination is closer to 1. The coefficient of determination is calculated by Pearson product moment correlation coefficient ([60]:

$$R^2 = \frac{\left[\sum\left(x-\bar{x}\right)\left(y-\bar{y}\right)\right]^2}{\sum\left(x-\bar{x}\right)^2 \sum\left(y-\bar{y}\right)^2} \tag{2-21}$$

Where x and y are position values in a coordinate system, $\bar{x}$ and $\bar{y}$ are mean of all x and y values. In this research, R^2 is used to illustrate the goodness of regression fitting results of curve of concentration against different impedance parameters.

The *Chi-Square* is the square of the standard deviation between the original data and the calculated spectrum. In this research, it is used to test the goodness of electrical circuit model fitting when the impedance spectrum is fitted by *Z-View*® software. It is defined as:

$$\chi^2 = \frac{\sum_{i=1}^{n}(X_i - \overline{X})^2}{\sigma_0^2} \tag{2-22}$$

Where σ_0^2 is the value of the population variance specified in the null hypothesis [59]. It is clear to see that the chi-square value is closer to zero if the fitting result is better.

2.6 Biological Application of EIS

2.6.1 Impedance Analysis on Plant Tissue

Impedance characterization of plants is mainly based on the electrical impedance spectroscopy method. This method is widely employed in several biological tissues studies, for instance, apples, persimmons, nectarines, plant leaves and scots pine shoots. This section provides a review on impedance investigations on plants.

2.6.1.1 Impedance Analysis on Apples and Tomatoes

EIS has been applied on indication of fruit ripening of apples and tomatoes by Varlan et al. [48]. It has been found that as low-frequency resistance increased, constant phase angle increased, characteristic frequency decreased, and high-frequency resistance slightly increased in normal ripening process. Apart from these observed trends, fruit classification was considered to be very difficult using *EIS*, owing to the large individual parameter dispersion over the whole population. In contrast, tomato classifications were more promising, due to the thinner skin and juicier flesh [48]. The variations of impedance parameters confirmed the tendencies observed from apple measurements. Green colour and red colour tomatoes were differentiated well by the low frequency resistance and the constant phase angle. The Hayden Model was used to interpret data. It was observed that the signal mainly comes from peel with the increase in low frequency resistance. In addition, skin extracellular resistance increases with ripening, and cell uniformity also increases in ripening [48, 61]. Liu [62] also reported that the apple sweetness can be indicated by *EIS*, which may replace the traditional *Brix* measurement.

2.6.1.2 Impedance Analysis on Nectarines

Impedance measurements were used to characterize changes between extracellular and intracellular resistance during cool storage and normal fruit ripening in nectarines [39, 52]. It is demonstrated that tissue resistance at 50 Hz has strong linear correlations with fruit texture, which is assessed by flesh firmness. The low frequency resistance was also closely related to the apparent juice content.

Electrical models allow analysis performed at the cellular level. Nectarine fruit tissues conform to the double-shell model. The magnitude of tissue block impedance was greater than the whole fruit, which indicates that each mini-circuit inside whole tissue connects in parallel, and that the current travels indirectly between two electrodes [39, 52]. Low frequency resistance of nectarines increased with the time stored in cool condition, and decreased during normal ripening. A similar change pattern has been observed from the previous peach study [63].

2.6.1.3 Impedance Analysis on Persimmons & Kiwifruit

Electrical impedance spectroscopy has been applied in persimmons [8]. The arc represented in the Nyquist Plot displayed a semicircular shape. They dilated gradually for the first 21 days, but contracted with further ripening. Resistance at 50 *Hz* in this study reflects the electrical properties of extracellular space, and resistance at 300 *kHz* reflects the properties of all tissue compartments [8]. In addition, the double-shell model fits data very well compared with the *Hayden* model and the model proposed by Zhang et al. [64]. Cytoplasm resistance of persimmon fruit was significantly lower when undergoing chilling, but it showed a rapidly increasing trend when fruit were transferred to room temperature for ripening [8].

Impedance investigation on kiwifruit did not indicate good relationships between impedance changes and physiological events [37]. There was little change in the impedance characteristics of the fruit during ripening, although firmness decreased by 10-fold. Apoplast resistance and total tissue resistance varied from one year to the other. It is suggested that the mobility of electrolytes inside the cell wall did not change during kiwifruit ripening through electrolyte leakage analysis. The physicochemical interactions taking place within the cell wall may have a major impact on the tissue impedance [37].

2.6.1.4 Impedance Analysis on Woody Plants

The impedance spectra of fruit, vegetable and plant leaves contain a typical single semicircular circle with its centre depressed below the *x*-axis [6, 48, 53]. However, the shapes of impedance spectra of woody samples vary. For instance, the

spectrum function of shoots and wood of the Scot pine is composed of two arcs, whilst the spectrum for the bark has only one arc, which shows a strongly depressed centre [65]. The three organs of Scot pine have different characteristics, it is suggested different models should be applied to them.

2.6.2 Impedance Analysis on Food Quality Assessment

The value of electrical impedance analysis depends on being able to relate the electrical impedance correctly to the physical or physiological properties of the observed sample [64]. Various environmental factors such as temperature and humidity will strongly affect the physiological status of fruit and vegetables. It has been demonstrated that impedance measurement is capable of reflecting rapid changes when the objective has any physical damage, such as that caused by chilling and bruising. Furthermore, impedance observations can be connected to the physiological changes of food. This section reviews the relevant applications of impedance measurement to food quality assessment.

2.6.2.1 Impedance Analysis on Bruising Damage in Food

Bruising can be caused anywhere during harvest, transportation and uploading. It is defined as damage to plant tissue by external forces which results in physical changes in texture and/or eventual chemical alteration of colour and flavour [7]. It is not only a cosmetic problem, but also it alters the functioning of plant cells [66]. Cell wall-digesting enzymes are free to digest the complex molecules of the cell wall when they are outside of the plasmalemma. As a result, the cell wall is weakened and fruit becomes soft. Bruising can lead to uncontrolled action of cell wall-digesting enzymes, so that the quality can be badly affected [66].

There are a few indirect methods to assess the bruising in agricultural products, such as X-ray and gamma ray transmission [7], nuclear clear magnetic resonance [67], and electrical impedance characteristics [7, 68, 69]. Impedance measurement provides a rapid method to detect the internal bruising of fruit without waiting for tissue browning as evidence of this. The magnitude of bruised tissue impedance is significantly lower than normal tissue, and the impedance spectra of bruised tissue displays two or more overlapped peaks compared with a single peak in the

unbruised tissue. Therefore, a bruised index is defined according to these phenomena [7]. Jackson et al.[69] found that the impedance difference before and after bruising at 50 Hz has good correlation with bruise weight. All the measurements and the calculations of the volume fraction of intact cells were significantly affected by cultivar. It is further found that the ratio of the extracellular resistance to the intracellular resistance has been reported to depend on the degree of the bruise only [68].

2.6.2.2 Impedance Measurement on Chilling Damage

Chilling damage is primarily a disorder of crops of tropical and subtropical origin. The injured fruit becomes dry, mealy, woolly, or like leather. There is flesh or pit cavity browning and flesh bleeding or internal reddening [70]. Flesh tissue separation and cavity formation are accompanied by the advanced stage of chilling damage. These symptoms are frequently observed from peach cultivars [70]. Chilling damage manifests in increased ion leakage [71], and rigidified cell wall [72]. Therefore, chilling damage limits the marketing and consumption of agricultural products.

Low frequency resistance exhibits a clear decrease in tomatoes due to solute leakage caused by injury [48]. Resistance of cytoplasm is the only parameter that indicate chilling damage in persimmons in one out of the five components of the double-shell model [8]. But it increases rapidly when fruit is transferred to room temperature for ripening. The cytoplasm resistance follows the same trend in nectarines with that of persimmons. However, there is a further reduction when fruit is removed from cool storage [52].

2.6.2.3 Other Applications Based on Electrical Impedance Analysis in Food

EIS also challenges traditional sensory methods, bacteriological assessment and the relevant chemical component analysis to determine fish freshness [73]. It was reported that the phase angle change with frequency is dependent on the storage time after kill. Rapid liquefaction of fish tissue due to deterioration increases the conductivity [73]. Therefore, impedance can also be employed as an indicator of

freshness. Moreover, referred changes in impedance have been used as indicators of shrimp freshness [74].

Apart from the application to seafood products, the impedance method has also been tried for meat quality assessment [46]. Freywald et al. [46] introduced a parameter *Py*, defined as the relationship between the conductivity of the extracellular and the intracellular pathway, which should be in good agreement with the quality of fresh meat.

2.6.3 Conclusion

The studies discussed above are applications to food assessment methods based on *EIS*. Until now though, impedance researches have been carried out in many foods and food products, research on wine quality control and production control by *EIS* methods are hard to find. Impedance properties of wines and other alcoholic beverages are still not researched previously. It is necessary to explore the impedance properties of wine and the possibility for using them as a tool to improve wine production.

Chapter 3
Electrical Impedance Spectroscopy Analysis on Pure Solutions

3.1 Introduction

As a pre-product of wine, grape musts contain a variety of components which will be changed or unchanged during fermentation. Sugar, which is one of the major parts of grape musts, is a group of soluble carbohydrates, including glucose, fructose, sucrose, etc. From fresh grape juice to wine by fermentation, carbohydrates decrease from about 25% (*w/w*) to 0.2%. However, at the same time, ethanol concentration increases to about 12% while it was zero in fresh grape juice. As another important component in grape must, tartaric acid is relatively unchanged during the fermentation, while malic acid is consumed by lactic bacteria during the lactic-melodic fermentation. The concentration of tartaric acid is 2~15 *g/L*, while malic acid concentration changed from 2~10 *g/L* to 0~2 *g/L* during the fermentation. [75]

As described in Chapter 2, ethanol content can be measured by traditional methods like density measurement, Ebulliometer, Alcohol Refractometer, as well as modern methods, such as Gas Chromatography (*GC*), High Performance Liquid Chromatography (*HPLC*), etc. Currently, these analytical chemistry techniques, including *GC* and *HPLC*, are prevalently used as an accurate measurement for ethanol content in fermenting grape must. However, the disadvantage of these methods is obvious, as it is normally a tedious process requiring expensive lab equipment. Traditional methods like density measurements are used in small wineries more common for cheap devices and easy operating. However, these methods can be influenced easily by many variations so that the low accuracy could lead to the high risk of fermentation failure. Recent reports show that new methods, like ultrasound based measurements [4], shortwave-near infrared spectroscopy and microwave based measurements [5], are under development. These methods have their advantages

including rapid measurement and high accuracy. On the other hand, their disadvantages are also clear, for example, ultrasound travelling through the fermentation tank will cause false reading of sound speed.

In this chapter, electrical impedance measurements are carried out on solutions with single solvent. The samples in these experiments include ethanol solutions, tartaric acid solutions and malic acid solutions. Resistance, reactance and impedance magnitude value are measured and discussed in these experiments. Furthermore, the Nyquist semi-circle diameters of ethanol solutions are also analysed. In this research, equivalent electrical circuit models are developed for ethanol solution and organic acid solutions to simulate the transmission of electrons between the electrodes.

3.2 Methodology

3.2.1 Sample preparation

All solutions were prepared with distilled water (*DI*) ($18M\Omega cm$). Ethanol solutions were prepared by dissolving the different volumes of absolute ethanol (Sigma, Germany, Analytical Grade, $0.789g/mL$, 99.5%) into distilled water. Different amounts of Tartaric acid (Sigma, Germany, Analytical Grade, 99 %) and DL-Malic acid (Sigma, Germany, Analytical Grade, 99%) is dissolved into distilled water to make acid aqua solutions. All solutions are prepared under room temperature and stored in a refrigerator under $4°C$ after preparation. Samples were moved into a constant temperature incubator 12hrs before the impedance measurement to restore the experimental temperature of $20°C$.

3.2.2 Electrodes Setup

The experiment was carried out inside an electrical cell with two platinum covered stainless steel electrodes. The reason why the platinum coated stainless steel electrodes was chosen is that the stainless steel electrodes have polarization property which will cover the impedance signal under low frequency. And according to previous tests, platinum coated stainless steel electrodes provide lowest polarization compare to other electrodes. The electrical cell is shown in Figure 3-1. These oblong-shaped electrodes, which have a size of $25mm \times 10mm$, were integrated on a polymer substrate. The distance between these two electrodes was $40mm$. All electrodes were cleaned with distilled water and absolute ethanol twice, and then dried under open air before use.

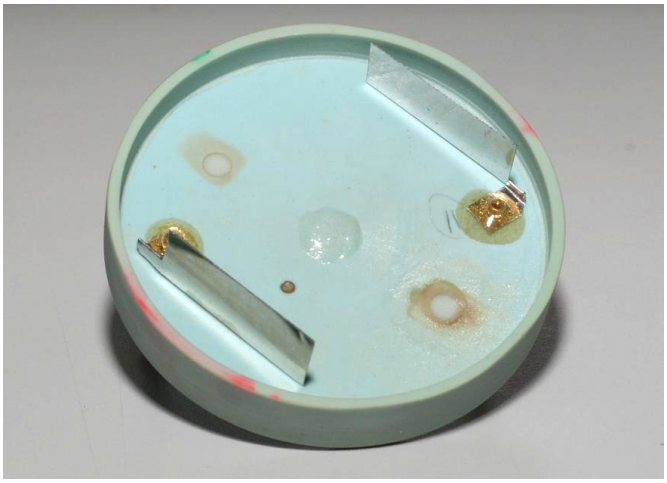

Figure 3-1 Electrodes fixed on a polymer substrate. It is a part of the electrical cell for EIS measurements.

3.2.3 Impedance measurements

The *EIS* was measured by a *Solartron*® 1260A Impedance/Gain-phase Analyser (Solartron Analytical, Hampshire, UK) connected with a *Solartron*® 1294 bio-impedance interface (Solartron Analytical, Hampshire, UK). (Figure 2-2) *Solartron*® 1260A provides a frequency sweeping range from 1 *Hz* to 10 *MHz* with an accuracy of 0.1% for magnitude and 0.1° for phase measurements. A desktop personal computer is used to control the impedance analyser and interface as well as to collect the measured impedance spectra via an *IEEE-488 GPIB* cable (National Instrument, USA). The *EIS* data were recorded using the *SMaRT*® software (Solartron Analytical, Hampshire, UK). 10*ml* solution samples were introduced to the electrochemical cell which was kept at a constant temperature of 20°*C*. After the impedance analyser was preheated and standardized with the standard impedance test module, an alternating current with amplitude of 100*mV* was applied to the cell over a frequency range between 1*Hz* to 1*MHz*. 31 spot frequencies were scanned for the impedance measurement. The experiment was carried out inside a Faraday cage to reduce the electromagnetic interferences.

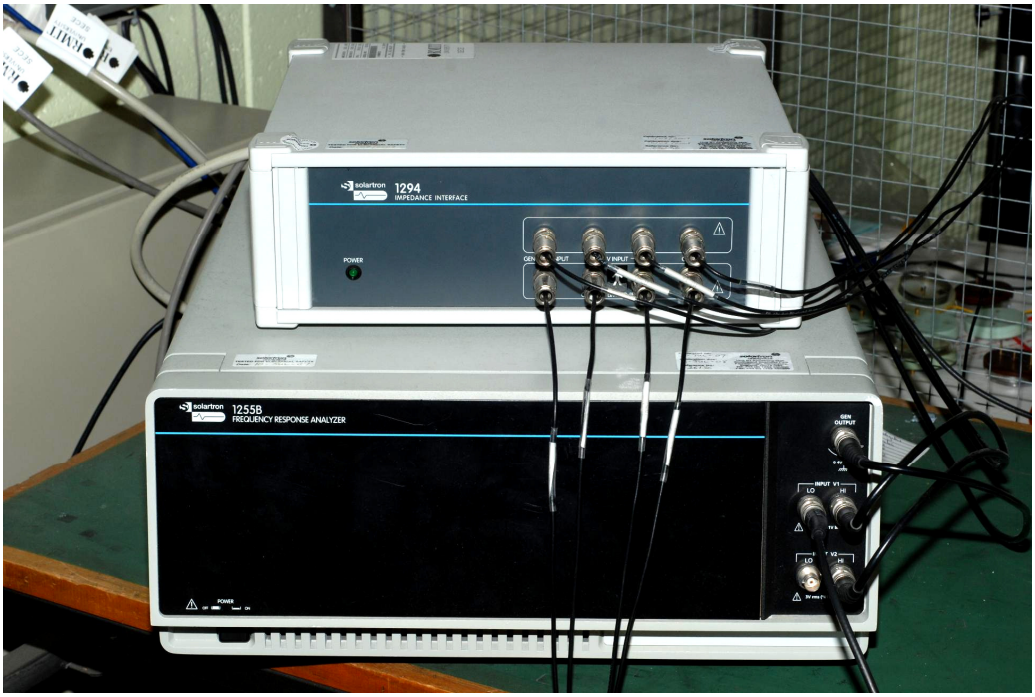

Figure 3-2 *Solartron*® 1260A Impedance/Gain-phase Analyser and *Solartron*® 1294 bio-impedance interface used in *EIS* measurements.

15 different ethanol solution concentrations were prepared as standard samples for Ethanol ranging from 2% to 30% *v/v* and with an equal difference of 2%. The Impedance measurement was performed 60 seconds after the complete infusion of the samples. The measurement of each solution sample took about 100-150 seconds. Each sample was measured three times to get an averaged impedance spectrum for further analysis. The cell including the electrodes was rinsed with distilled water and dried after each measurement.

Two types of organic acids, tartaric acid and malic acid, with 4 different concentrations each, are used as samples in this research. Similar to ethanol experiments, each sample was measured three times and average impedance spectrums are output. The concentrations of ethanol and organic acids pure solutions tested in *EIS* experiments are listed in Table 3-1.

Table 3-1 Concentrations of pure ethanol and organic acids solutions used in EIS measurements.

Solution Types	Concentrations							
Ethanol (%v/v)	2.0	4.0	6.0	8.0	10.0	12.0	14.0	16.0
	18.0	20.0	22.0	24.0	26.0	28.0	30.0	
Malic Acid (g/L)	2.0		4.0		6.0		8.0	
Tartaric Acid (g/L)	2.5		5.0		10.0		15.0	

3.3 Results and discussion

3.3.1 Impedance Properties of Ethanol solutions

Resistance and reactance were calculated from the measured impedance and phase angle. As mentioned in Chapter 1, there are two ways to illustrate the impedance data, Bode plots and Nyquist plot. The Bode plots, which are impedance magnitude and phase angle against frequency, are one of the effective tools for showing conductivity of solutions at different frequencies. As an example, bode plot of 2% ethanol pure solution is shown in Figure 3-3.

It can be clearly seen that impedance magnitude value is constant near 1800$k\Omega$, while it begins to decrease when the frequency reaches to $10^{3.6}$ Hz. And the phase angle variety starts to be existed in the frequency range $10^{2.6}$ to $10^{4.8}Hz$.

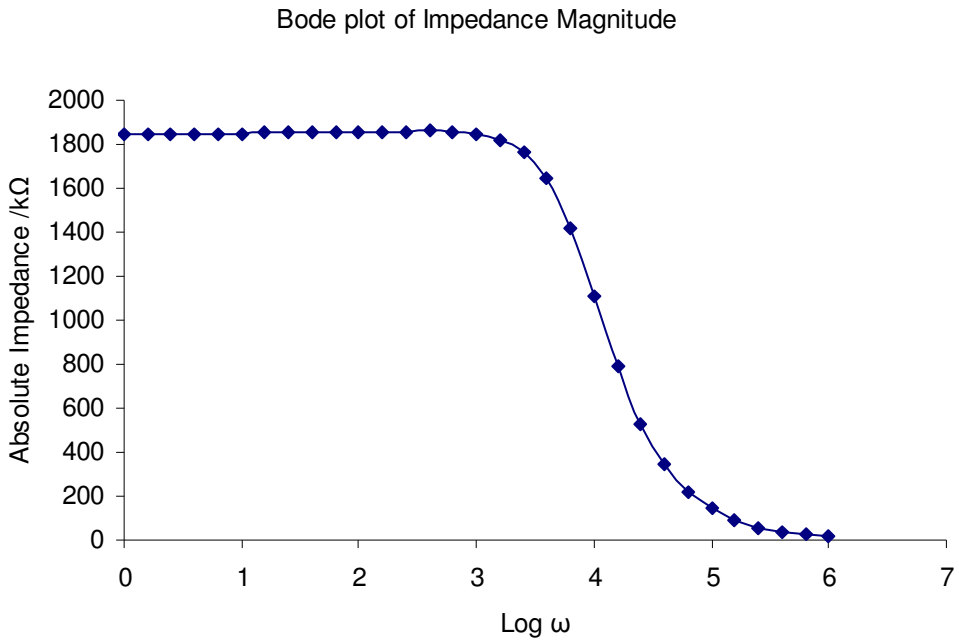

Figure 3-3a

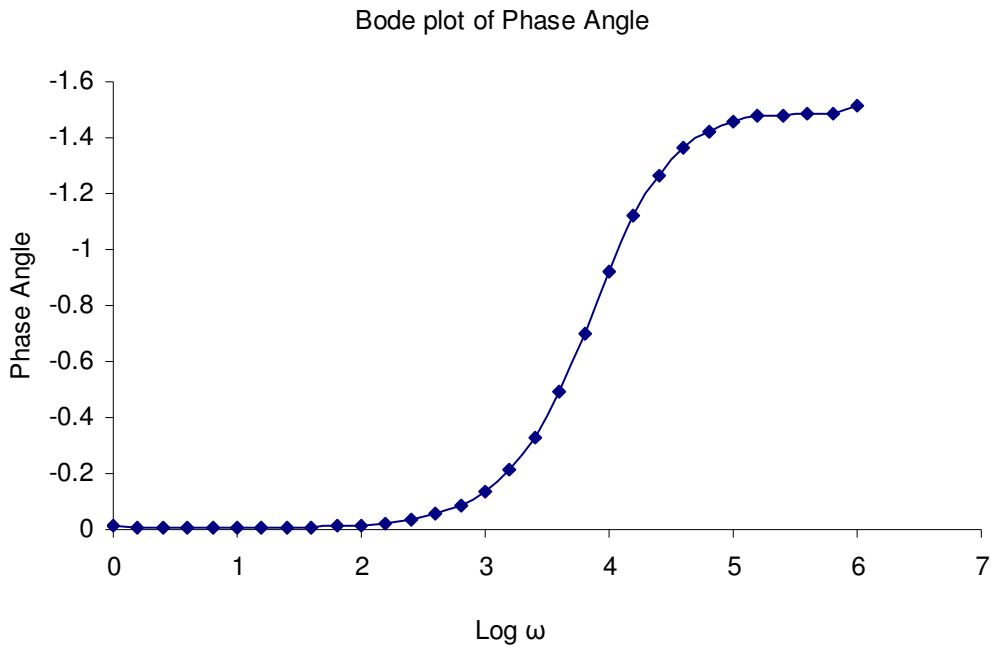

Figure 3-3b

Figure 3-3 The bode plots of 2% ethanol solution. (a) the bode plot of impedance magnitude; (b) the bode plot of phase angle.

Nyquist Plots of all samples are illustrated in Fig.3-4. The spectra of the ethanol solutions with different concentrations all have a nearly perfect semi-circle shape. The centers of those semi-circles are all below the *X*-axis. The reactances are normally minus values, in order to locate the Nyquist plot in 1st quadrant of the coordinate system, the minus-reactance is used. So in this thesis, all the reactance mentioned are minus-reactance, except for those which are noticed.

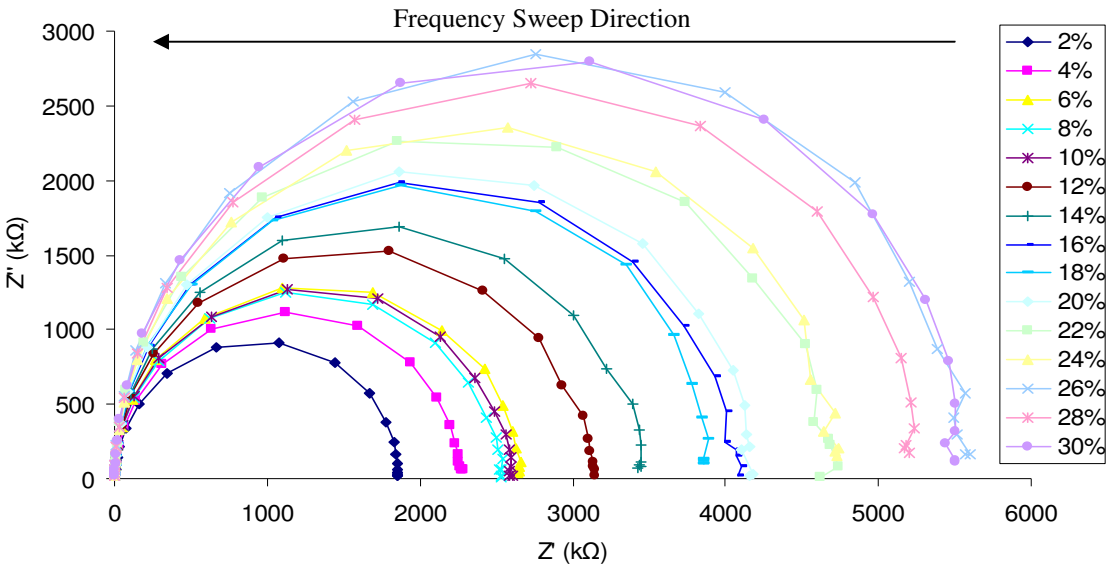

Figure 3-4 The Nyquist plots of ethanol solutions with a concentration range of 2% to 30%. The frequency sweep direction is shown. The Nyquist plots are not semi-circles as they appear. In fact, they are part of circles which have the circle centre in the 4th quadrant of the coordinate system.

As Bode plots and Nyquist plots are two effective methods of impedance data analysis, they both have their advantages. The Bode plots display impedance magnitude and phase angle variety with frequency change. And the Nyquist plots shows clearer relationship of resistance and reactance than that of bode plots. As Nyquist plot contains more information of impedance variation under whole frequency, it is mainly used for *EIS* data analysis in this research.

Though the Faraday cage has been used for removing the electrical noise interference, unstable points can still be seen within the low frequency ranges (<100*Hz*). This is due to the electrode polarization impedance caused by the electrochemical reaction which occurs in the contact interface between electrodes and tissue.

The Polarization of a sample is the electric dipole moment density, the mean electric dipole moment of the molecules, multiplied by the number density. The electrode polarization impedance (*EPI*) is generally believed to be caused by the

rough electrode surface and the ion infiltration and absorption process [54]. Harker and Maindonald [52] reported that the *EPI* can be many times larger than the sample impedance at low frequencies therefore could lead to inaccuracies in the measurement. For this reason, low frequencies between 1 *Hz* to 60*Hz* were not considered as effective data.

3.3.1.1 Single Frequency Impedance

It can be seen from Fig. 3-4 that the semi-circle diameter changes with the variation of the ethanol solution concentrations. The frequency at the highest reactance point is around a range from $10^{3.2}$ to $10^{3.6}$ *Hz* for these Nyquist plots. By this reason, a specific point at $10^{3.6}$ *Hz*, is chosen to reveal and compare the features of single frequency impedance of different concentrations.

Fig.3-4 shows the relationship of impedance magnitude (|*Z*|), real part resistance (*Z'*) and imaginary part reactance (*Z"*) against solution concentration at $10^{3.6}$ *Hz*. The formulae fitted by using linear regression for impedance magnitude, reactance and resistance are:

$$C = 1.86\times10^{-7}\times|Z| - 0.30 \tag{3-1}$$

$$C = 1.48\times10^{-7}\times Z'' - 0.10 \tag{3-2}$$

where *C* is the concentration of ethanol solutions, and |*Z*| is the impedance magnitude, *Z"* is the reactance and *Z'* is the resistance.

According to the Figure 3-5(a) and (b), both |*Z*| and *Z"* have good linear correlation with ethanol concentration. Especially the reactance *Z"*, which has a coefficient of determination (R^2) of 0.9668. However, the resistance *Z'* has shown no clear correlation at all with the ethanol concentrations.

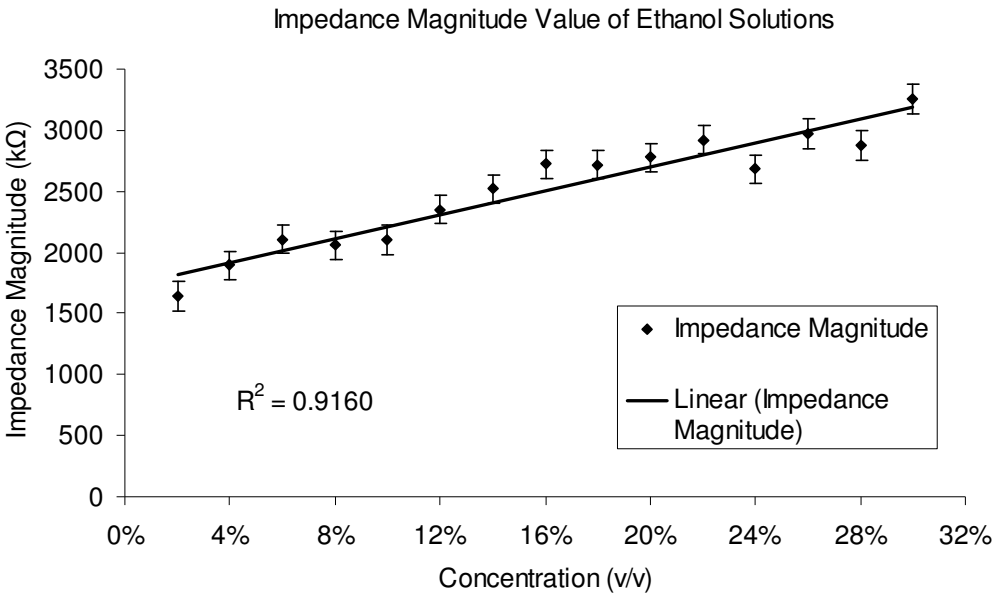

Figure 3-5a

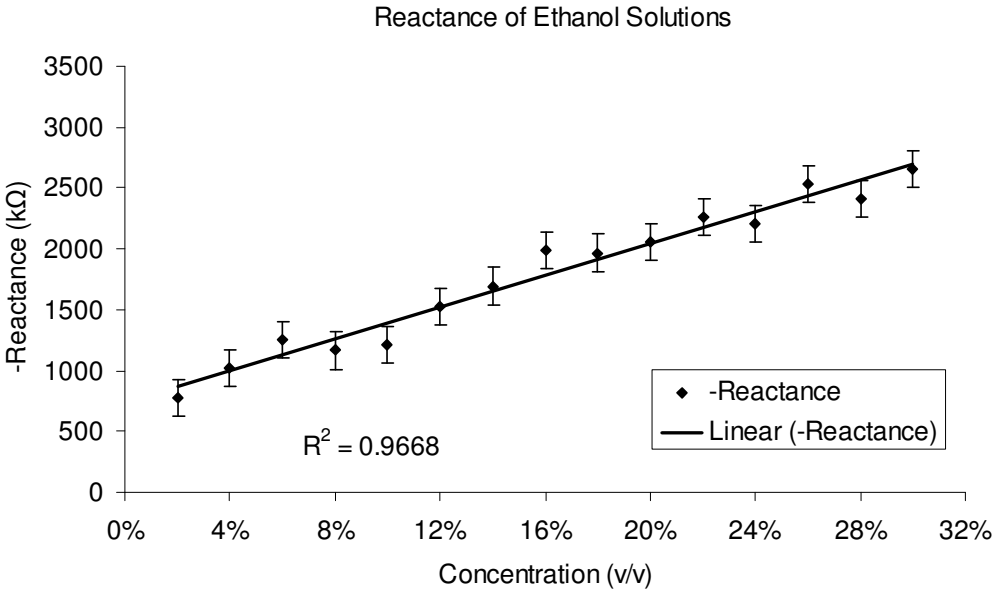

Figure 3-5b

Figure 3-5 Comparison of the impedance magnitude and its imaginary part (reactance) at $10^{3.6}\ Hz$ against the ethanol concentration. The linear coefficient of determinations (R^2) is shown. (a) Impedance magnitude value; (b) minus value of reactance;

As analysed, the single frequency impedance analysis provides a shortcut to present the corresponding value when the concentration is unknown. The single frequency measurements are much easier to carry out than multiple frequency measurements. Compared to the resistance value and impedance magnitude value, the reactance value is more applicable to indicate the ethanol concentration as its higher accuracy.

3.3.1.2 Diameter of the Nyquist Semi-circle

As the Nyquist plot for ethanol solution is shown as a closed perfect semi-circle, the diameter of the fitted semi-circle can be used as a feature to characterize the obtained impedance spectra. The diameter and circle centre positions of the Nyquist semi-circle are fitted by *Z-View*® software (Scribner Associates Inc., 2005). The diameter shows good correlation with ethanol concentration, while the circle centers scattered randomly. The mean diameter and standard deviation (σ) as well as coefficient of variation (*Cv*) are calculated and listed in Table 3-2.

Table 3-2 The mean diameters of Nyquist circle on samples of different concentration

Concentration	Mean Diameters	σ	*Cv*
2%	1.91×10^6	66997.34	3.51%
4%	2.27×10^6	328882.20	14.49%
6%	2.53×10^6	251033.60	9.94%
8%	2.57×10^6	63772.59	2.48%
10%	2.53×10^6	61871.56	2.45%
12%	3.13×10^6	72800.00	2.33%
14%	3.51×10^6	73022.62	2.08%
16%	3.97×10^6	99013.45	2.49%
18%	4.03×10^6	174770.80	4.33%
20%	4.27×10^6	460405.00	10.79%
22%	4.53×10^6	267390.10	5.90%
24%	4.82×10^6	53501.12	1.11%
26%	5.51×10^6	167887.70	3.04%
28%	5.32×10^6	145886.60	2.74%
30%	5.61×10^6	37424.37	0.67%

The linear correlation between concentrations and diameter of Nyquist circle shows clearly in Fig.3-6. The R^2 of this equation is 0.9796, which indicates a strong linear correlation with the diameters and the correlation equation is in Eq. 3-4:

$$C = 7.27 \times 10^{-8} \times D - 1.10 \tag{3-4}$$

where C is the concentration and D is the diameter of circle in Ω.

Compared with the specific frequency point analysis, diameter analysis provides better linear relationship with the concentration as its higher coefficient of determination. However, diameter analysis needs a *Z-View*® program to fit the semicircle, which may enlarge the error and complicate the data processing procedure.

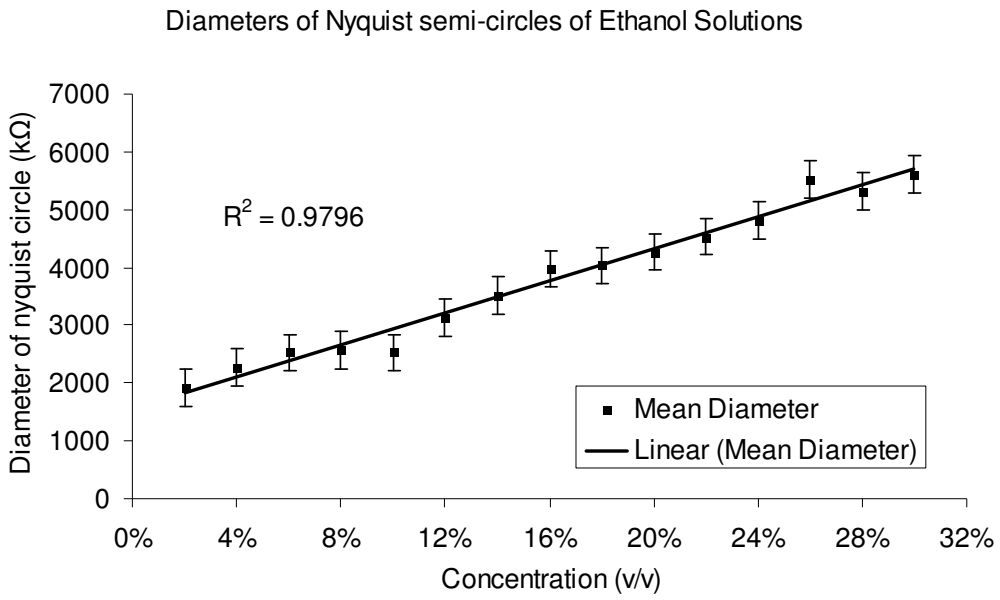

Figure 3-6 The concentration vs. mean Diameter of the Nyquist circle. The coefficient of determination of this equation is 0.9796, which shows high linear correlation with the diameters.

The dielectric response of a pure resistor-capacitor parallel circuit has a perfect semicircle whose circle centre is on the resistance axis and radius equals to the half value of the resistance in the *R-C* circuit. That means the diameter can characterizes the impedance properties of sample ethanol solutions. However, though the Nyquist plots of ethanol solutions are similar to that of the *R-C* parallel circuit, they are not the same. This is because the circle centers of ethanol solutions are located below the resistance axis and the radius is not exactly half of the resistance. Thus more sophisticated systems than a pure *R-C* parallel circuit are required to model the dielectric properties of ethanol solutions.

3.3.1.3 Equivalent Electrical Circuit for Ethanol Solutions

Single frequency impedance and diameter of Nyquist semi-circle provide two effective tools to analyze impedance properties of ethanol solutions. These two methods have such advantages as easy operation and simple calculation process. However, previous research [54, 55] suggests that constant phase-angle element provides better results when an equivalent electrical circuit is applied. In this research, this method is tested and discussed.

Figure 3-7 shows an equivalent electrical circuit, where a resistance paralleled with a *CPE*, was chosen in this work. Compared with the electrical models which were established by previous researchers (e.g. the *Cole* model, the *Hayden* model and double-shell model), this model has a better fitting result and lower chi-square values. The *Rs* is the solution resistance and the *CPE* is the distributed component in the solution. In this case, the impedance is calculated as:

$$Z = \frac{1}{\frac{1}{Rs} + T(j\omega)^{\phi}} \tag{3-5}$$

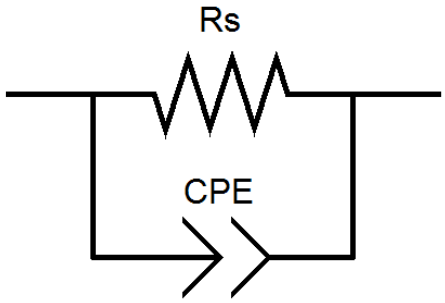

Figure 3-7 The equivalent electrical circuit, which is used to simulate the electrical cell in ethanol solution research. It consists of a resistance parallel with a *CPE*.

The *Z-View*® software was used to fit the impedance arc. As can be seen in Figure 3-8, Nyquist plots, as well as Bode plot, were fitted to the equivalent electrical circuit. The Bode plot consists of two subplots, the Bode magnitude plot which is a graph of log magnitude against log frequency, and the Bode phase plot which is a graph of phase against log frequency.

The fitting result, including values of components and errors were output from the software. With these values, the impedance fitting result of each sample is given by equation 3-5. For example, the impedance of 2%v/v ethanol solution is:

$$Z_{0.2} = \frac{1}{5.34\times10^{-7} + 1.61\times10^{-11}(j\omega)^{0.9704}} \tag{3-6}$$

Similarly, impedance formulae of 15 ethanol solutions with different concentrations are fitted. A *Chi-square* value, which is the square of standard deviation between the original data and the calculated spectrum, was obtained to define the goodness of fitting. That means the chi-squared value closer to zero, the fitted impedance curve closer to measured curve.

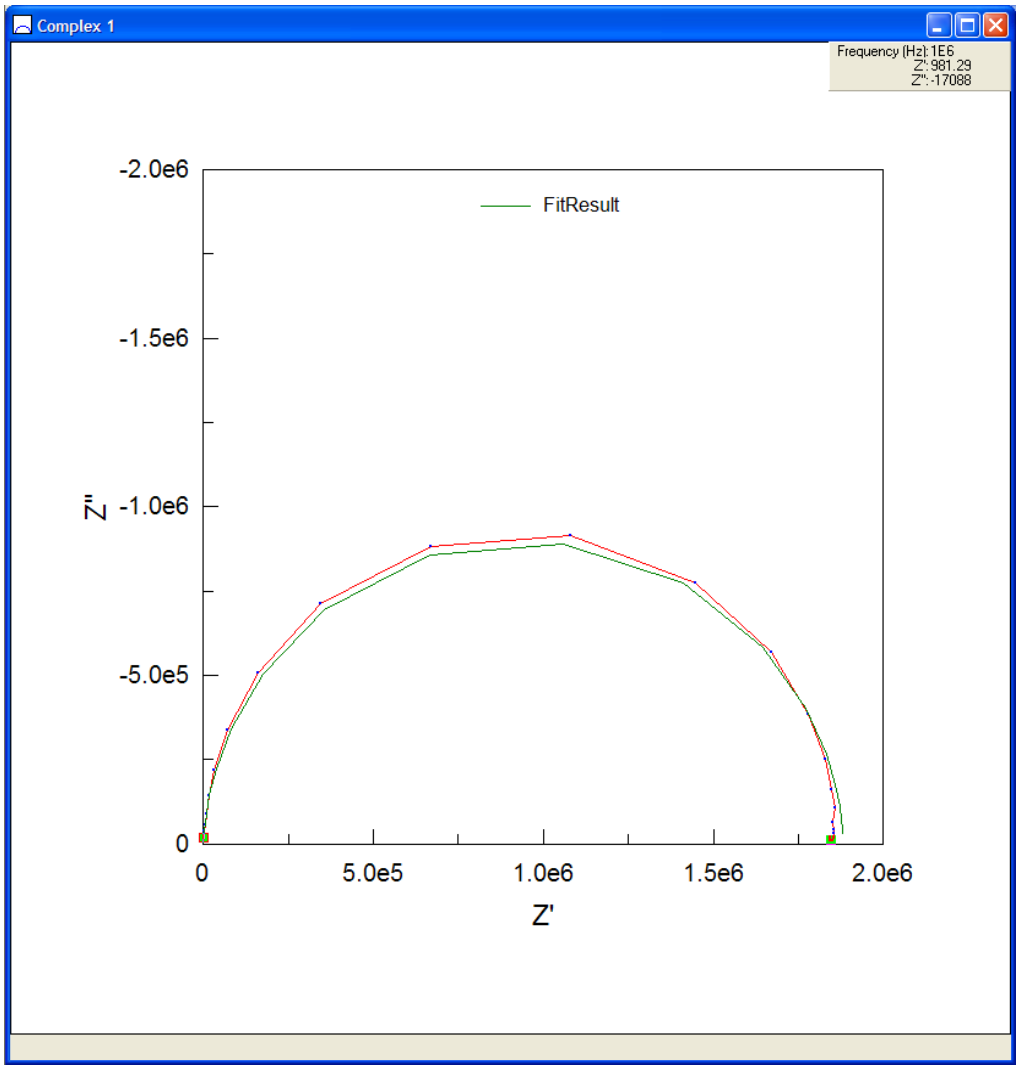
Complex 1
Frequency (Hz):1E6
Z':981.29
Z'':-17088
FitResult
-2.0e6
-1.5e6
-1.0e6
-5.0e5
0
Z''
0
5.0e5
1.0e6
1.5e6
2.0e6
Z'

Figure 3-8a

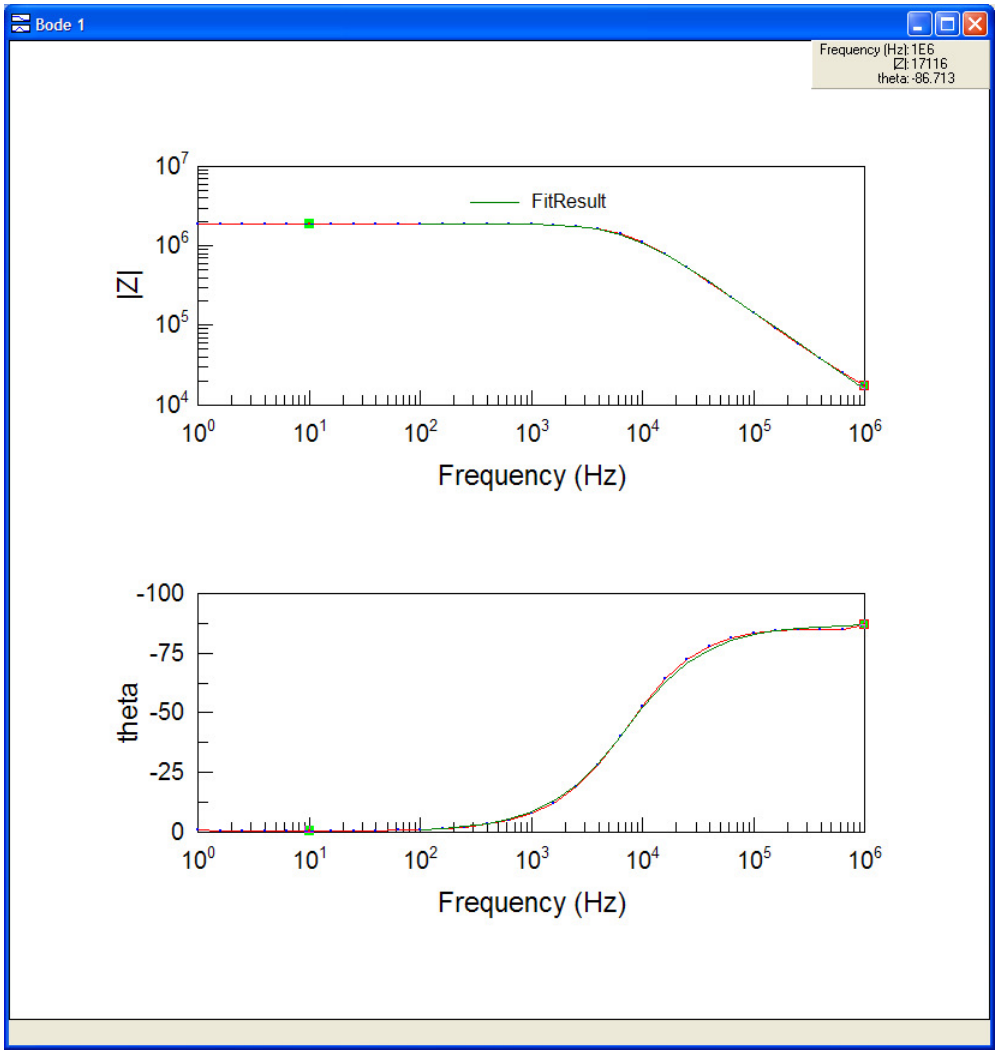

Figure3-8(b)

Figure 3-8 Fitted Nyquist plot and bode Plots. The impedances spectrum (red line with blue points) was fitted to the equivalent electrical circuit, which contains the solution resistance and the constant phase element. The ideal impedance spectra obtained from the fitting (green line in the plot). (a) Nyquist plot; (b) Bode plots

The calculated values and errors for each element of the equivalent circuit are shown in Table 3-3. The *CPE-P* value is the Φ in Equation 3, which is usually between 1 and 0.5 [76]. The *CPE-P* value is related to the angle of rotation of a purely capacitive line on the complex plane plot. That means, when the *CPE-P* is 1.0 the *CPE* can be considered as a pure capacitor.

Table 3-3 fitted result obtained from *Z-View*® software for each element of the equivalent circuit, including *Rs, CPE-T, CPE-P* and *Chi-square*.

Con.	*Rs*	*CPE-T*	*CPE-P*	*Chi-Square*
2%	1.87×10^{6}	1.61×10^{-11}	0.970	0.003037
4%	2.29×10^{6}	1.63×10^{-11}	0.968	0.003933
6%	2.68×10^{6}	1.56×10^{-11}	0.973	0.003698
8%	2.56×10^{6}	1.55×10^{-11}	0.971	0.004549
10%	2.63×10^{6}	1.53×10^{-11}	0.971	0.004179
12%	3.16×10^{6}	1.52×10^{-11}	0.972	0.004978
14%	3.49×10^{6}	1.43×10^{-11}	0.974	0.004060
16%	4.12×10^{6}	1.46×10^{-11}	0.973	0.005317
18%	4.00×10^{6}	1.40×10^{-11}	0.976	0.004628
20%	4.25×10^{6}	1.42×10^{-11}	0.975	0.003395
22%	4.75×10^{6}	1.39×10^{-11}	0.976	0.004547
24%	4.83×10^{6}	1.56×10^{-11}	0.978	0.003368
26%	5.74×10^{6}	1.46×10^{-11}	0.978	0.004474
28%	5.40×10^{6}	1.49×10^{-11}	0.977	0.003769
30%	5.72×10^{6}	1.32×10^{-11}	0.976	0.004752

Table 3-3 indicates that *Rs* value increases monotonously along the increase of ethanol concentration, whereas *CPE-T* keeps relative constant. The reason is that *CPE-T* is a constant related to the sample dimension. The samples in this study were treated as liquid cuboids, which can be considered as a three-dimensional distribution. According to previous researches, *CPE-T* parameter has no important influence on sample capacitance [56]. However, the *CPE-P* value, which is known as the Φ parameter of *CPE*, is related to the absolute *Z"* value in the Nyquist plot. *CPE-P* value demonstrates a parameter of proximity to resistance or capacitance. When *CPE-P* is 1, this element performs as a pure capacitor. While *CPE-P* is 0, it performs as a pure resistor. Hence, if the ethanol solution is considered as a capacitor, the concentration of ethanol must show strong

capacitive performance. That means, the higher concentration, the closer the *CPE* to a capacitor. The fitting results confirmed this as shown in Figure 3-8.

The linear correlations of *CPE-P* and *Rs* against solution concentration are illustrated in Fig.3-9. The *Rs* value shows a strong linear correlation which has a coefficient of determination of 0.9733. The *CPE-P* value shows an unstable wave under the low concentration solutions which lowers the coefficient of determination to 0.8124. Thus, *CPE-P* is not a reliable parameter at low solution concentrations.

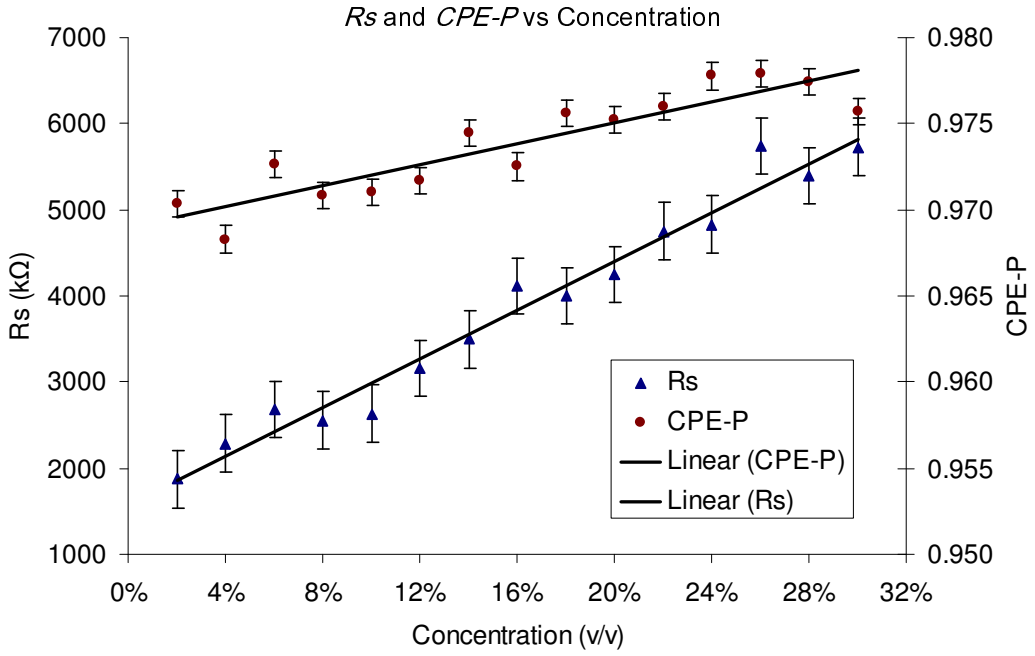

Figure 3-9 *Rs* and *CPE-P* vs. Solution Concentration.

As Rs is calculated using whole impedance spectra from 60*Hz* to 1*MHz*, it reveals the virtual resistance of the whole distributed sample. Consequently, this equivalent electrical circuit model can be applied in many dielectric solutions.

3.3.2 Electrical Impedance Properties of Organic Acid Solutions

3.3.2.1 Impedance Spectrum of Tartaric acid and Malic acid

Wine acidity influence many factors during the fermentation, such as solubility of tartrate salts, the effectiveness of sulphur dioxide, ascorbic acid, enzyme additions, the solubility of proteins, effectiveness of bentonite, the polymerization of the colour pigments as well as the oxidative and browning reactions [17]. Essentially, wine acidity is mainly relevant to the concentration of organic acids. There are two major organic acids in grape juice, tartaric acid and malic acid. In this section, tartaric acid and malic acid pure solutions are investigated. Whereas the tartaric acid concentration in grape must is under 10 *g/L* [13], tartaric solutions in the range of 2.5~15 *g/L* is simulated as the acidity solution. Malic acid has a content which ranges from 1.0-8.0 *g/L* in grape must [17]. In this work, impedance properties of malic acid solutions in the range of 2.0~8.0*g/L* are investigated. Unlike dielectrically solutions (such as ethanol solutions), tartaric acid and malic acid solutions have full conductivity on the surface of electrodes, which means that it is not polarizable. As shown in Figure 3-10, Instead of a nearly perfect semicircular found for ethanol which indicates a strong capacitive nature, a series of oblique lines with a similar slope were discovered within the low frequency range (1-100 *Hz*) while the imaginary part (the reactance) is close to zero within the high frequency range (100 *Hz* – 1 *MHz*). This is due to the abundance of free ions in the acid solution which makes its dielectric properties more resistive. Furthermore, the positions of the oblique lines change with the acidity concentration.

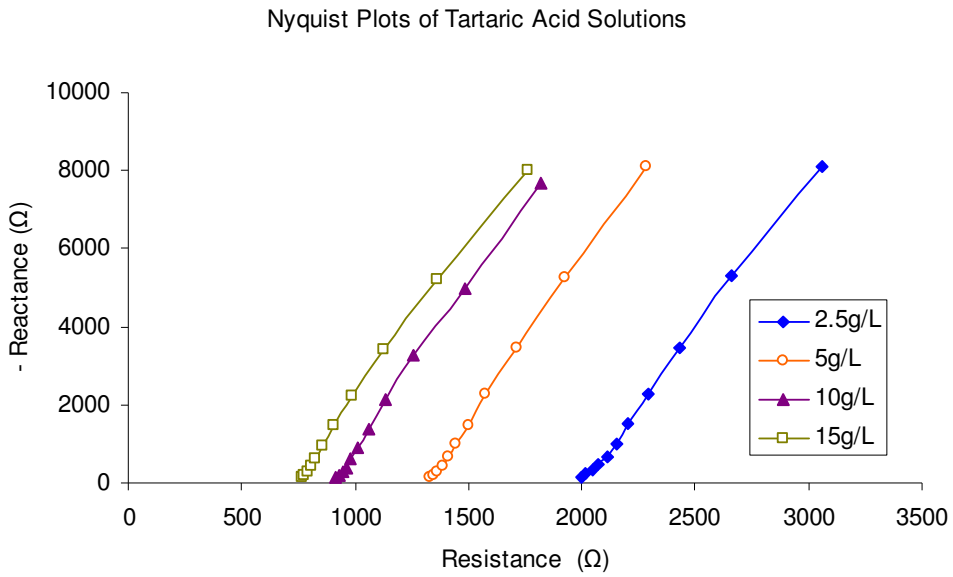

Figure 3-10a

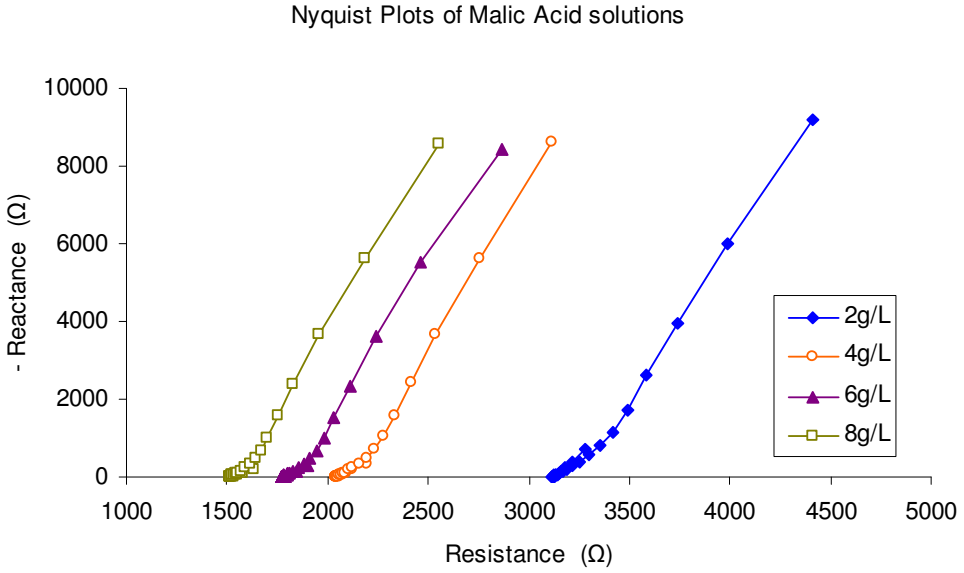

Figure 3-10b

Figure 3-10 Nyquist plots of organic acid solution. The measured points under 1~100Hz are shaped as oblique lines, while the reactances under frequencies above 1 kHz are close to zero. (a)Nyquist plot of tartaric acids; (b)Nyquist plot of malic acids.

The *EPI* which smears the impedance measurement in the low frequency range for ethanol is not a problem for acid solutions due to the availability of the free ions. However, because the capacitive reactance of the solution reduces quickly with the increase of the excitation frequency, the *EPI* becomes evident in higher frequency range (>100 *Hz* in this case). Thus different to the ethanol solution for which the frequencies higher than 60 *Hz* are considered, frequencies from 1 *Hz* to 60 *Hz* for these two organic acid solutions are researched.

3.3.2.2 Equivalent Electrical Circuit Fitting for Organic Acid Solutions

The *Z-View*® software was applied to fit both Nyquist plot and Bode plot by an equivalent electrical circuit. Distinct from the ethanol solutions, acidity solutions have low impedance which is caused by the free ions. Thus, the solution should be considered as a resistor instead of a distributed element. Nevertheless, the *EPI* still exists all the time even if it is not evident from 1*Hz* to 60*Hz*. In order to remove the influence of *EPI* and other electrode impedance, a *CPE* is used in the equivalent electrical circuit in acid solutions. Therefore, the fitting electrical model is a resistance connected with a *CPE* in serial. The resistance (*Rs*) in the serial circuit is the simulation of solution resistance.

Table 3-4 Fitted results obtained from *Z-View*® software for each element of the equivalent circuit, including *Rs*, *CPE-T*, *CPE-P* and *Chi-square*.

Solution Type	Con. (g/L)	*Rs*	*CPE-T*	*CPE-P*	*Chi-Square*
Tartaric Acid	2.5	2007.7	2.2779×10^{-5}	0.9155	0.000392
	5.0	1332.0	2.2595×10^{-5}	0.9225	0.000311
	10.0	916.5	2.3675×10^{-5}	0.9261	0.000270
	15.0	757.2	2.2853×10^{-5}	0.9273	0.000210
Malic Acid	2.0	3207.7	2.0353×10^{-5}	0.9079	0.000646
	4.0	2095.7	2.1449×10^{-5}	0.9146	0.001158
	6.0	1817.0	2.1844×10^{-5}	0.9198	0.000569
	8.0	1572.3	2.1108×10^{-5}	0.9255	0.000419

In Table 3-4, *Rs, CPE-T, CPE-P* values are listed. It is interesting that though *CPE-P* values are the properties of *EPI*, it has an increasing trend with the increase of acid concentration. With *MATLAB* Curve Fitting Toolbox, power correlations between *CPE-P* and the concentration are found (3-7, 3-8), which have R^2 of 0.9758 for tartaric acid and 0.9504 for malic acid. However, the exponents are very high (72.52 for malic acid and 134.14 for tartaric acid). Furthermore, it is evident again that the *CPE-T* is a constant which corroborates the assumption made by this model.

$$C = 2384.99 \times CPE_P{}^{72.52} \tag{3-7}$$

$$C = 3.14 \times 10^5 CPE_P{}^{134.14} \tag{3-8}$$

In this model, *Rs* is defined as the resistance of solution. It can be seen in Table 3-4, the *Rs* values reduce with the increase of concentration in both tartaric acid and malic acid. It is reasonable as the conductivity of solution is contributed by ions in the acid fluids. The higher the ion concentration, the more free ions can transmit the current and the lower the resistance. In order to analyse the relationship between acid concentration and *Rs* value quantification, the following theoretical deduction is made.

The conductivity of electrolyte solutions is caused by ions which can be dragged through the solvent by the application of a potential difference between two electrodes[77]. Here, the conductance of solution is defined as *G*. The conductance of solution is equal to $R/(R^2+X^2)$, where R is the resistance and X is the reactance. However, in acid solutions, the mainly reactance is caused by EPI and electrode impedance. The actual reactance of solution is much smaller than resistance. In this case, G can be defined as the inverse of its resistance *R*, so:

$$G = R^{-1} \tag{3-9}$$

And, *G* decreases with the length (ℓ) of electrolyte and increases with its cross-sectional area (*A*), suppose that $n = A/\ell$, then,

$$G = \kappa n \tag{3-10}$$

Where κ is the conductivity.

A molar conductivity is defined as the conductivity divided by the molar concentration (c):

$$\Lambda_m = \frac{\kappa}{c} \tag{3-11}$$

In weak electrolytes, such as Malic acid or Tartaric acid, as they are diprotic acids, it has equilibrium in the solution:

$$H_2A(aq) + H_2O(l) \leftrightarrow H_3O^+(aq) + HA^-(aq) \qquad (Ka_1) \tag{3-12}$$

$$HA^-(aq) + H_2O(l) \leftrightarrow H_3O^+(aq) + A^{2-}(aq) \qquad (Ka_2) \tag{3-13}$$

Where Ka_1 and Ka_2 are acidity constants, which are the chemical equilibrium constants of ionization equilibriums. Then the total acidity constant in the solution is:

$$K_a = K_{a1}K_{a2} \tag{3-14}$$

As the ionization extent of reaction 3-13 is much smaller than that of 3-12, it can be ignored. This means, the Ka_1 is approximately equal to Ka.

Therefore, the degree of ionization (α), which is the proportion of solute ions concentration in the solutions, can be:

$$\left[H_3O^+\right] = \alpha c \qquad \left[HA^-\right] = \alpha c \qquad \left[H_2A\right] = (1-\alpha)c \tag{3-15}$$

Then, the Ka is approximately

$$K_a = \frac{\alpha^2 c}{1-\alpha} \tag{3-16}$$

The acid is fully ionized at infinite dilution, and infinite dilution molar conductivity is defined as Λ^o_m

Consequently, the measured molar conductivity Λ_m is given by:

$$\Lambda_m = \alpha\Lambda^\circ_m \tag{3-17}$$

From (3-7) and (3-8):

$$\kappa = (nR)^{-1} \tag{3-18}$$

From (3-9) and (3-15):

$$\frac{\kappa}{c} = \alpha\Lambda_m^\circ \tag{3-19}$$

From (3-16) and (3-17):

$$\alpha = \left(nRc\Lambda_m^\circ\right)^{-1} \tag{3-20}$$

With (3-16), (3-20) can be reformed as:

$$c = \left(n^2\Lambda_m^{\circ 2}K_a\right)^{-1}R^{-2} + (n\Lambda_m^\circ)^{-1}R^{-1} \tag{3-21}$$

As *Ka* is normally a very small value, e.g, Malic acid has a *pKa* of 8.53, which means the *Ka* of malic acid is $10^{-8.53}$. Therefore, the coefficient of R^{-2} will be much bigger than that of R^{-1}. So practically, R^{-1} term can be ignored.

Then, in pure weak acid solutions, the relationship between concentration and resistance is:

$$c = \left(n^2\Lambda_m^{\circ 2}K_a\right)^{-1}R^{-2} \tag{3-22}$$

As *n*, $\Lambda^o m$, and *Ka* are all constants, the concentration of acid has power correlation with the solution resistance. For convenience, the coefficient of equation 3-20 is defined as a resistance-concentration constant (γ). So the equation can be reformed as:

$$c = \gamma^{-1}R^{-2} \tag{3-23}$$

According to the deductions above, a power correlation exists between the concentration and the *Rs* value. This relationship is applied to the fitting of *Rs* and concentration. *MATLAB*® Curve Fitting Toolbox is used for power fitting. Figure 3-11 shows the fitting result of both tartaric acid and malic acid.

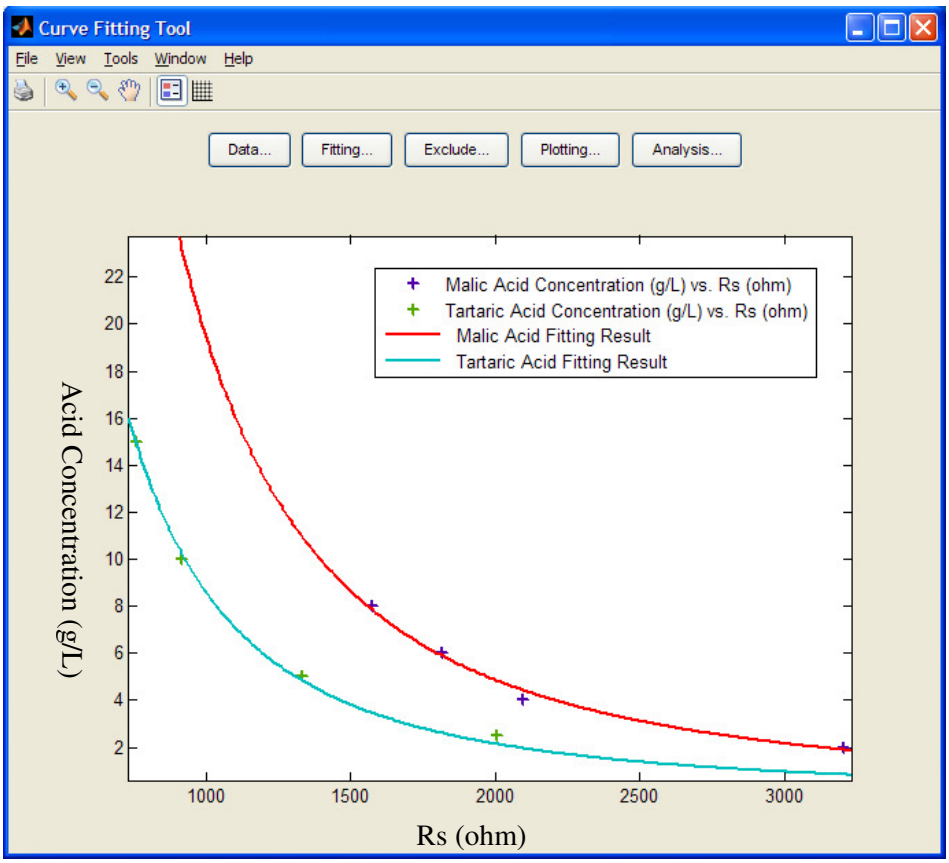

Figure 3-11 The fitting results of organic acids concentration and *Rs* value in *MATLAB*® Curve Fitting Toolbox.

As can be seen, the results fit the theoretical model quite well. For tartaric acid, the fitting result is very close to the theoretical value as its R^2 is 0.9977. The R^2 of malic acid fitting, which is 0.9884, is also high as well. Equations 3-21 and 3-22 illustrate the formulae of the curves of *Rs* against concentration.

$$c_{TA} = 8.578 \times 10^6 \times Rs^{-2} \tag{3-24}$$

$$c_{MA} = 1.945 \times 10^7 \times Rs^{-2} \tag{3-25}$$

According to the above formulae, the γ^{-1} value of the fitting formula of malic acid (1.945×10^7) is larger than that of tartaric acid (8.578×10^6). It also makes sense because both $\Lambda^o m$ and *Ka* of tartaric acid are larger than that of malic acid. Based on the equation 3-20, as the coefficient has a negative exponent of -1, the larger constants mean a smaller γ^{-1}.

3.4 Conclusion

Research on pure solutions, which provide basic electrical impedance properties for ethanol, malic acid and tartaric acid solutions, is presented in this chapter. As the discovery of high correlation between solvent concentration and impedance parameters, the concentration of major components of grape juice under fermentation (ethanol, tartaric acid and malic acid) are confirmed suitable to be measured by *EIS* in their aqueous solutions. The relationships between concentration of these constituents and impedance parameters (impedance magnitude of specific frequency, diameter of Nyquist semi-circle and the *Rs* and *CPE* value of equivalent electrical circuit) are clear and reliable.

Ethanol solutions show high impedance values. In this case, the Nyquist plot which shaped a semi-circle provides enough information to find the concentration. Three data analysis methods are compared and tested for confirmation of their reliability. Firstly, the impedance magnitude and reactance of specific frequency shows good correlation with the ethanol concentration. The R^2 of impedance magnitude against concentration is 0.9276, and that of reactance against concentration is 0.9668. Though the goodness is not high enough for high precision measurement, such a method is still applicable as its simple operating and quick response.

Secondly, diameter of Nyquist semicircle shows better correlation with ethanol solutions concentrates as the higher R^2 of 0.9796. However, diameter analysis needs analysis software such as *Z-View*® to fit the semicircle to derive the diameter value, which may complicate the data processing procedures.

The equivalent electrical circuit model is also applied to the analysis of Nyquist plot. With *Z-View*® software, each electrical component in a virtual circuit with a resistance (*Rs*) and a parallel *CPE* is fitted. The *Rs* illustrates a highly linear relationship with the concentration, where the R^2 is 0.9733. The linear relationship between the concentration and *CPE-P* value is relatively lower, where the R^2 is 0.7509.

According to the reliability and other features, these three methods have their own advantages and applications. Though the veracity of impedance magnitude of specific frequency method is slightly lower than that of the diameter of Nyquist semicircle, it may be accepted by those who do not need high precision but a quick and cheap device. The diameter of Nyquist semi-circle method takes longer operating time and more complex data analysis, but it is the most reliable method for data analysis compared with others. The equivalent electrical circuit method needs a complicated analysis process. However, it is not able to improve the performance of ethanol concentration measurement. The fitting result suggests that a different model may need to be developed for the equivalent electrical circuit method.

EIS method applied on measurements of concentrations of tartaric acid and malic acid pure solutions are also investigated in this chapter. Compared with ethanol solutions, tartaric acid and malic acid solutions show different impedance properties. The Nyquist plots of acid solutions show an oblique line. In order to analyse the impedance property of these organic acid solutions, an *Rs-CPE* serial model is designed to fit the *EIS* outputs. As the *CPE* simulates the electrode impedance which is combined with the *EIS* signal, the *Rs-CPE* model removes the impact of *EPI* and electrode impedance effectively. According to the theoretical deduction, the solution resistance has power correlation with the concentration. The reliability of the correlation is extremely high as the R^2 value is up to 0.9884 for malic acid and 0.9977 for tartaric acid. These results suggest that *EIS* is a high precision method for organic acid concentration measurements. In order to find out whether this method is valid for separate concentrations of tartaric acid and malic acid in their compound solutions, and whether the ethanol could influence the ionization of these organic acids, the next chapter will illustrate the investigations of *EIS* analysis on compound solutions.

Chapter 4
Electrical Impedance Spectroscopy Analysis on Compound solutions

4.1 Introduction

Based on previous research, relationships between impedance properties of pure solutions and their concentration are found. A further step for compound solutions research is necessary as wine is a complex solution containing all these compounds mixed. The research on impedance properties of compound solutions explores the potential of *EIS* to separate the different solvents.

Rare reports are found in research of impedance properties of compound solutions. Rocha and Simoes-Moreira [78] reported that an impedance sensor was developed for determining ethanol and regular gasoline mixtures mass content. Grafov and Damaskin [79] demonstrated a generalized theory with a combination of Onsager mutual relationship and Gibbs absorption equation for mixed electrolyte solutions. The Acid Dissociation Constant (*pKa*) of hydroxyl-benzophenones in ethanol-water mixtures is determined by Castro et al. [80]. Their research also reported the ethanol could alter the *pKa* value of weak organic acid in water solutions. All these researches suggest that the reciprocity of the solvents in the compound solution largely influences their impedance properties.

As discussed in Chapter 2, during the wine fermentation, there are two major changes happening. The first one is called ethanol fermentation, in which almost all the sugar from the grape juice is transformed into ethanol. In the malolactic fermentation, malic acid content keeps reducing until the malic acid is totally consumed by lactobacillus. Practically, a decision of fermentation end point is usually important for winemaking, as latter or earlier stop of fermentation probably cause a fermentation failure. Traditionally, the judgment of the fermentation stages depends on the experience of the winemaker. However, in large wineries, the objective judgment by winemakers is not reliable due to the

poor reliability of human sensory. A subjective tool needs to be used to monitor the fermentation stages of both ethanol fermentation and malolactic fermentation.

In this chapter, the impedance property of 4 types of compound solutions is discussed. Equivalent electrical models are confirmed to be suitable for compound organic acid solutions. The *Rs* value of compound solutions is found to have power correlation to the *Rs* value of each compound in pure solution condition. The electrical impedance of organic acids in ethanol-aqua solutions is also investigated. As a result, the ethanol can influence the ionization of organic acid solutions. These discoveries are obviously helpful for further research on *EIS* applications on real grape fermentation.

4.2 Methodology

4.2.1 Sample Preparation

Similar to single solvent solutions, compound solutions are prepared by distilled water at room temperature. Three types of compound solutions are prepared by using absolute ethanol (Sigma, Germany, Analytical Grade, 0.789g/mL, 99.5%), sucrose (Sigma, Germany, Analytical Grade, 99%), Tartaric acid (Sigma, Germany, Analytical Grade, 99 %) and DL-Malic acid (Sigma, Germany, Analytical Grade, 99%). Solid reagents are measured with an analytical balance (0.0001g, The Mettler-Toledo, Switzerland) and dissolved into a small amount of distilled water in volumetric flasks. Veracious amounts of ethanol are moved to the volumetric flasks by pipettes. The flasks are then filled up with the distilled water, and shaken in order to mix the solvents well. The concentrations of compound solutions are listed in Table 4-1.

Table 4-1 Concentration of compound solutions, including malic acid, tartaric acid, ethanol and sucrose. (Continued Overleaf)

Concentration of MA, TA, Ethanol and Sucrose in Compound solutions					
Solution Type	Solution No.	MA (g/L)	TA (g/L)	Ethanol (% v/v)	Sucrose (% w/w)
Ethanol and Sucrose compound solutions	1	-	-	0	24
	2	-	-	1	22
	3	-	-	2	20
	4	-	-	3	18
	5	-	-	4	16
	6	-	-	5	14
	7	-	-	6	12
	8	-	-	7	10
	9	-	-	8	8
	10	-	-	9	6
	11	-	-	10	4
	12	-	-	11	2
	13	-	-	12	0
Organic acids compound solutions	14	2	5	-	-
	15	4	5	-	-
	16	6	5	-	-
	17	8	5	-	-
Tartaric acid and Ethanol compound solutions	18	-	5	4	-
	19	-	5	8	-
	20	-	5	12	-
	21	-	5	16	-

Concentration of MA, TA, Ethanol and Sucrose in Compound solutions					
Solution Type	Solution No.	MA (g/L)	TA (g/L)	Ethanol (% v/v)	Sucrose (% w/w)
Organic acids and Ethanol compound solutions	22	8	5	2	-
	23	7	5	4	-
	24	6	5	6	-
	25	5	5	8	-
	26	4	5	10	-
	27	3	5	12	-
	28	2	5	14	-
	29	1	5	16	-

4.2.2 Impedance Measurements

The impedance measurements of compound solutions are the same as that of pure solutions. *Solartron* 1260A Impedance/Gain-phase Analyzer and *Solartron* 1294 Bioimpedance Interface are used to collect impedance data at a frequency range of 1Hz to 1MHz. *SMaRT* software is run for controlling the impedance analyzer, and the *Z-View*® and *MATLAB*® Curve Fitting Toolbox software operate the data fitting as well. All the impedance measurements are carried out under a temperature of 20°*C*. Each sample is duplicated three times to minimize equipment error.

Platinum coated copper electrodes are still used in compound solution measurements. The measurement procedures are the same as that of pure solutions. As sugar is used in these measurements, electrodes and containers are rinsed for three minutes with distilled water and dried until the surface of the electrodes are clean.

4.3 Results and Discussion

4.3.1 Impedance Properties of Sugar and Ethanol Mixtures

Based on experiments of ethanol-aqua solutions, impedance magnitude at specific frequency and diameter of Nyquist semicircles have been confirmed effective to measure ethanol concentration. In order to research whether the measurements can be applied to more complicated solutions, tests on solutions containing not only ethanol, but also sugar need to be carried out. The concentration of ethanol and sugar in these samples is based on the data of fermenting wine grape musts. In the series of samples, ethanol is added in a range of 0-12%*v/v*, while the sucrose is added in a range of 24-0%*v/v* in descending order.

Figure 4-1 shows the result of sucrose/ethanol compound solutions. Impedance magnitudes and reactance on $10^{3.6}$ *Hz* are also chosen for analysis. As can be seen in Fig.4-1(a) and (b), the impedance magnitudes and reactance are similar when the ethanol contents are lower than 6%. Then, the impedance rose quickly with the increase of ethanol concentration.

Figure 4-1(b) shows Nyquist plot diameters during fermentation. The curve is much smoother than that of impedance magnitude at $10^{3.6}$ *Hz*. Diameters of Nyquist plot are very close when ethanol content is less than 6%v/v. However, when the ethanol concentrations become higher, the increase of diameters become obvious. This may be because of the hydroxyl in sugar and ethanol. In ethanol or sugar solutions, the hydroxyl can be ionized into proton in very small quantities. As sucrose, glucose or fructose has 5 hydroxyls in each molecule, the ionization could be more obvious than that of ethanol, which contains only one hydroxyl. This fact leads to the increase of impedance magnitude when the ethanol concentration becomes high.

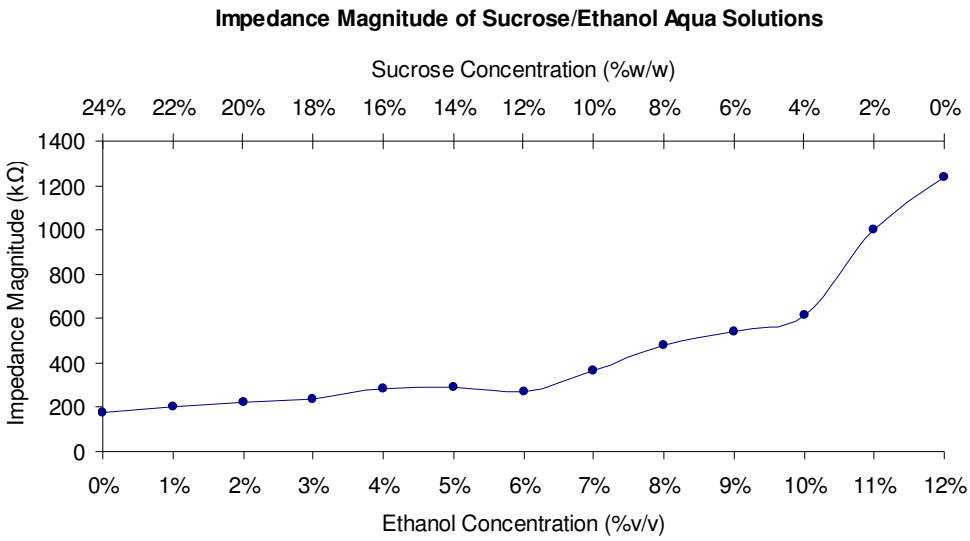

Figure 4-1a

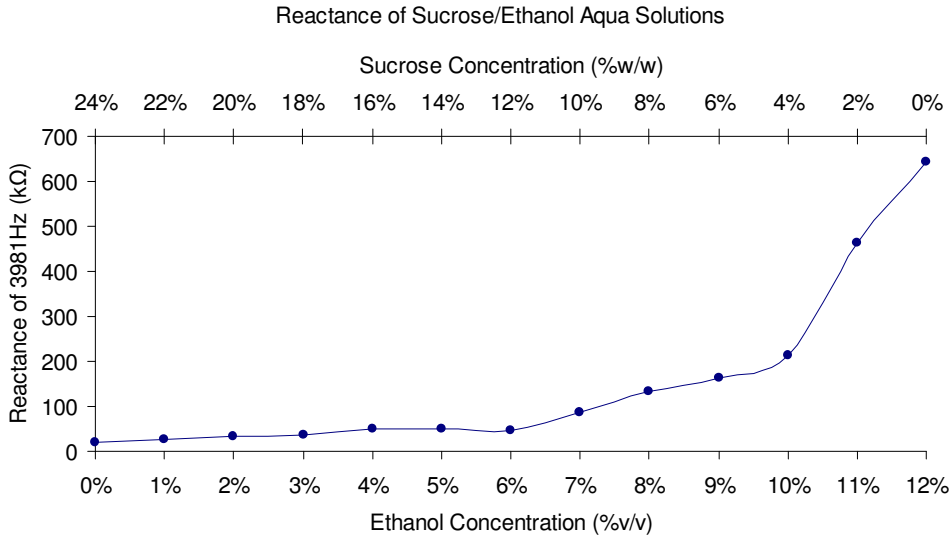

Figure 4-1b

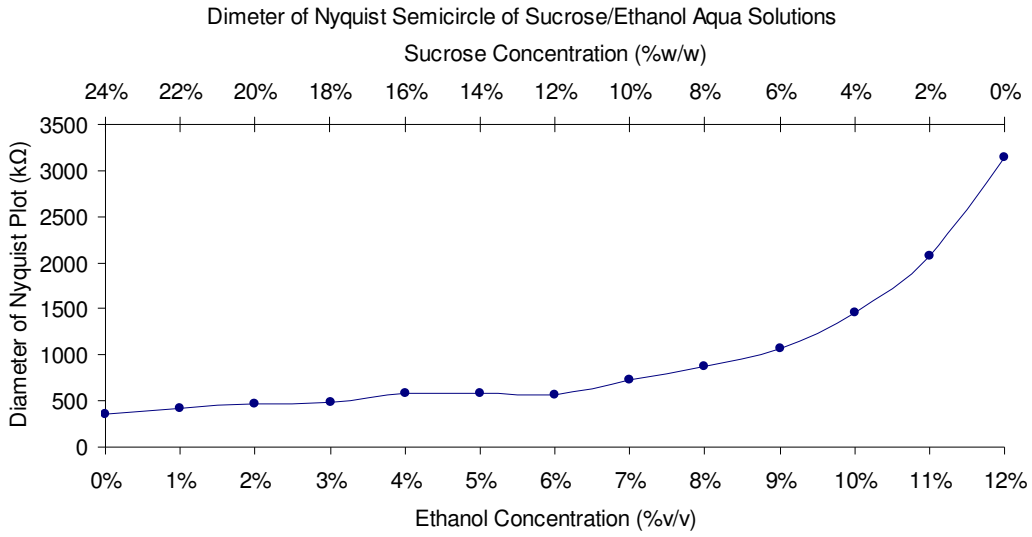

Figure 4-1c

Figure 4-1 The Impedance Magnitude and Diameter of Nyquist Semicircle against sucrose and ethanol concentration. (a) the Impedance Magnitude on 3981Hz vs Solvents Concentration; (b) the Reactance on 3981Hz vs. Solvents Concentration; (c) the Diameter of Nyquist Semicircle vs Solvents Concentration.

The results obtained from the sucrose-ethanol compound solutions test show that it is possible to use *EIS* methods to monitor the wine fermentation process, especially to indicate the termination of fermentation. The sugar in samples influence the value of electrical impedance. Before half the sugar is consumed by yeast, it would hide the impedance properties of ethanol. That's the reason why the impedance magnitude and diameter of Nyquist semi-circle have very small change when ethanol concentration is low. In low sugar content solutions, the extreme increase of impedance magnitude values point to full? fermentation termination. When the value of impedance magnitude reaches the top, the ethanol content in the grape must can be considered highest, and the fermentation process can be deemed finished. Though the single frequency method does not show ethanol content accurately, the benefit of this method is that it can get the result faster than any other impedance measurements.

4.3.2 Impedance Measurements of Organic Acid Mixtures

Electrical impedance spectroscopy of tartaric acid and malic acid mixtures is measured. Because the tartaric acid concentration remains relatively stable during the fermentation process, a concentration of 5*g/L* was chosen for this acid. Four different malic acid concentrations, 2.0 *g/L*, 4.0 *g/L*, 6.0 *g/L*, and 8.0 *g/L*, were chosen to mix with the tartaric acid to form 4 different tartaric and malic compound solutions to simulate the malic decrease process. The Nyquist plots are shown in Figure 4-2, in which the oblique lines are distributed more uniformly than that of pure solutions.

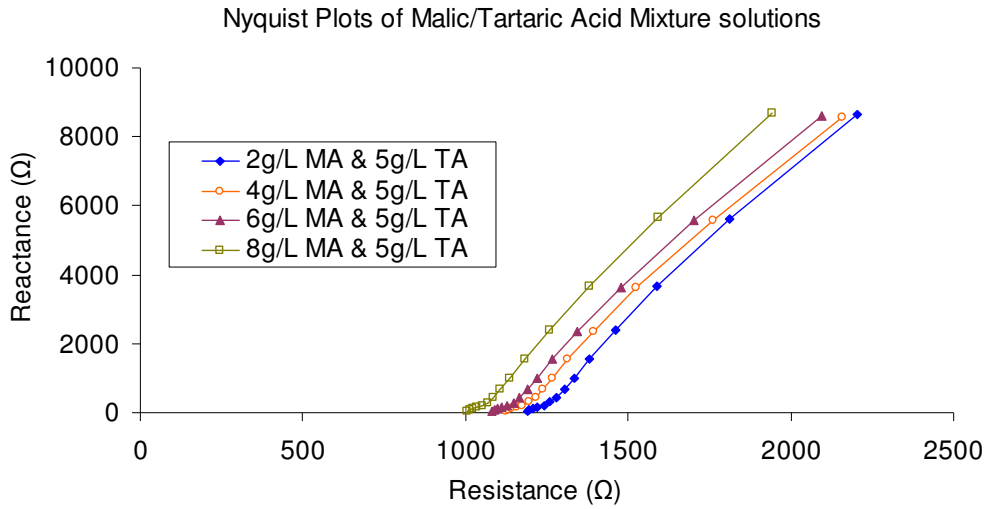

Figure 4-2 The Nyquist plots of Malic/Tartaric Compound solutions.

The same electrical model, which has a resistance (*Rs*) and a constant phase element (*CPE*) in serial, is used for analysis of pure organic acid solutions, was used for those compound solutions. The fitting results are listed in Table 4-2.

Table 4-2 Fitted results obtained from *Z-View*® software with the equivalent electrical circuit for malic and tartaric compound solutions.

Solution No.	Concentrations		*Rs (Ω)*	*CPE-T*	*CPE-P*	*Chi-Square*
	MA (g/L)	TA (g/L)				
1	2.0	5.0	1220	2.0838×10^{-5}	0.9291	0.000343
2	4.0	5.0	1156	2.0872×10^{-5}	0.9311	0.000464
3	6.0	5.0	1101	2.1024×10^{-5}	0.9493	0.000328
4	8.0	5.0	1032	2.0597×10^{-5}	0.9534	0.000339

Similar to pure solutions, the *CPE-P* values are showing an increasing trend with the increase of malic acid concentration. This is because the closer the *CPE-P* value is to zero, the closer *CPE* performs as a resistor. As the ion concentration of the compound solution increases, the increasing conductivity tend to perform more resistivity. However, the variation of *CPE-P* is not large enough to indicate the acid concentration well. So *Rs* value is mainly discussed in this work.

A power correlation between the *Rs* value of compound solutions and the malic acid concentration is found. Theoretically, this power correlation can also be analysed by the following deduction.

From equation 3-21, the relationships between pure solution concentrations of malic acid and tartaric acid are defined as:

$$C_{MA} = \gamma_{MA}^{-1} Rs_{MA}^{-2} \tag{4-1}$$

$$C_{TA} = \gamma_{TA}^{-1} Rs_{TA}^{-2} \tag{4-2}$$

As compound solutions have complicated ionization processes, in order to simplify the analysis procedures, a new coefficient (γ_m) of resistance-concentration may be defined:

$$C_m = \gamma_m^{-1} Rs_m^{-2} \tag{4-3}$$

And also, in the compound solutions, malic acid and tartaric acid are the only two solvents in this situation:

$$C_m = C_{MA} + C_{TA} \tag{4-4}$$

From 4-2, 4-3, 4-4, a relationship can be inferred:

$$C_{MA} = \gamma_m{}^{-1} Rs_m{}^{-2} - (\gamma_{TA}")^{-1} Rs_{TA}{}^{-2} \quad (4\text{-}5)$$

As the $\gamma_{TA}"$ and Rs_{TA} are constant as the concentration of tartaric acid not change, then equation 4-5 can be simplified to:

$$C_{MA} = \gamma_m{}^{-1} Rs_m{}^{-2} - \delta \quad (4\text{-}6)$$

Where δ is a tartaric acid factor, which is highly related to the concentration of tartaric acid in the compound solutions.

In equation 4-5, $\gamma_{TA}"$ is different to the γ_{TA} in single tartaric acid solutions, as the malic acid added in the compound solution may weaken the ionization and reduce the *Ka* value of tartaric acid, which means, the $\gamma_{TA}"$ is smaller than the γ_{TA}.

Under real conditions of wine fermentation, tartaric acid concentration is relatively constant. That means the δ value can be measured and remain at a constant level during the fermentation period. On the other hand, γ_m constant in equation 4-5 can also be measured in advance by a series of measurements in the laboratory.

Figure 4-3 displays the fitting result of organic acid compounds test according to the results listed in Table 4-3. The *MATLAB*® Curve Fitting Toolbox is used for fitting of the *Rs* value of compound solutions. As a result, the γ_m constant and the δ value are found. The fitting equation (4-6) forms a high R^2 value of 0.9798.

$$C_{MA} = 2.268 \times 10^7 Rs_m{}^{-2} - 12.99 \quad (4\text{-}6)$$

By using this equation, a concentration of malic acid can be measured directly by testing Rs_m value from *EIS* in organic acid compound solutions.

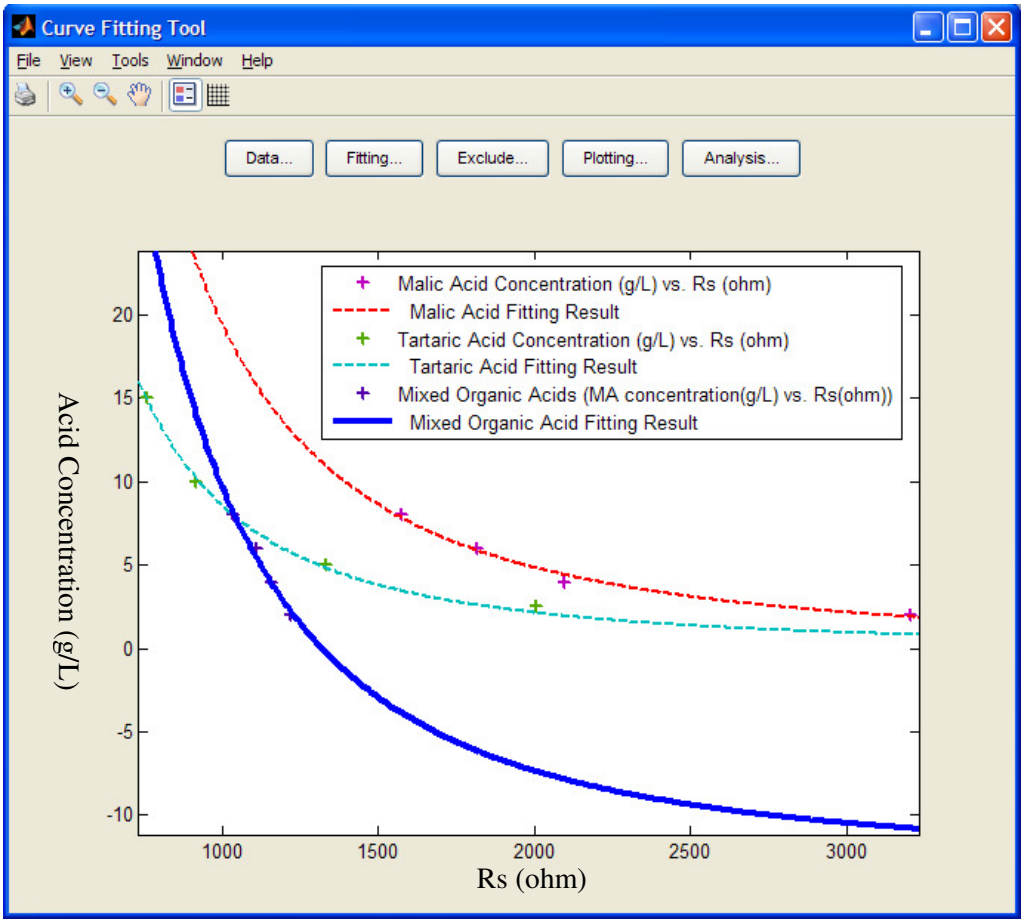

Figure 4-3 The fitting result of mixed organic acid (the blue line) by *MATLAB*® Curve Fitting Toolbox.

4.3.3 Impedance Measurements of Organic Acid and Ethanol Mixture

4.3.3.1 Tartaric Acid and Ethanol Compound Solution

During the grape must fermentation process, the ethanol concentration experiences an increase from almost zero at the beginning to around 12% while all sugar has been converted. Thus, it is necessary to understand the impedance properties of a solution mixed with organic acids and ethanol. In the first step, the impedance of tartaric acid and ethanol compound solutions are analysed.

As the tartaric acid has almost no change during the fermentation, 4 different concentrations of ethanol mixed with 5 *g/L* tartaric acid were prepared. The Resistance- *CPE* model is used in fitting the *EIS* results of these samples. Table 4-3 listed the fitting results.

Table 4-3 The fitting results of tartaric acid and ethanol compound solutions.

Concentrations		*Rs* (*Ω*)	*CPE-P*	*Chi-Square*
Tartaric Acid (*g/L*)	Ethanol (*%v/v*)			
5.0	4.0	1617	0.9224	0.000409
5.0	8.0	1935	0.9183	0.000445
5.0	12.0	2278.3	0.9129	0.000487
5.0	16.0	2685	0.9095	0.000479

According to the fitting results, the *CPE-P* value reduced with the increase of ethanol concentration. This may result from the ethanol increasing the capacitive nature of the electrodes as the lower *CPE-P* value means the closer the *CPE* performs as a capacitor. A linear relationship between ethanol concentration and *Rs* is also found. Equation 4-7 shows its linear correlation formula which has a high R^2 of 0.9968.

$$C_E = 0.01124Rs - 13.9274 \tag{4-6}$$

The finding of linear correlation suggests the ethanol may influence the ionization process. As a hydroxyl compound, ethanol weakens the ionization of tartaric acid, which reduces the amount of free ions in the solution. Naturally, the higher concentration of ethanol in the solution leads to less free ions being released by tartaric acid, which makes the higher solution resistance.

4.3.3.2 Malic Acid, Tartaric Acid and Ethanol Compound Solutions

In order to simulate the concentration variation during the fermentation process, the malic acid is added into tartaric acid and ethanol compound solutions. Thus a mixed malic acid, tartaric acid and ethanol aqua solution with 8 different concentrations were prepared. The ethanol concentrations are chosen from 2% *v/v* to 16% *v/v* and the malic acid concentrations are chosen from 8 *g/L* to 1*g/L*. Figure. 4-4 shows the Nyquist plot of eight such mixed acids and ethanol aqua solutions. It can be seen that the mixed acid solutions have similar straight lines (the left 4 oblique lines) as those found for pure acid solutions due to their high resistive nature. However, the Nyquist plots for the compound acid and ethanol solution, the right 4 lines, are slightly curved. Those curves can be seen as the

combination of the resistive straight oblique lines of acid solutions and the semi-circle contributed from ethanol. The fitted results are showed in Table 4-4.

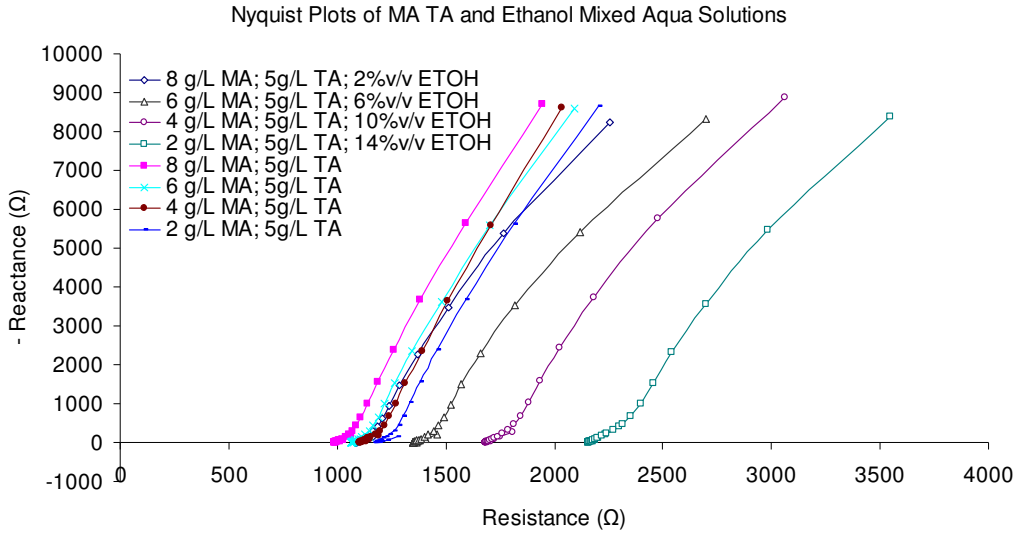

Figure 4-4 Nyquist plots of 8 mixed aqua solutions.

Table 4-4 Fitted results obtained from *Z-View*® software for Rs of mixed malic acid, tartaric acid and ethanol aqua solutions.

Concentration			*Rs (Ω)*	*CPE-P*	*Chi-Square*
TA (*g/L*)	MA (*g/L*)	ET (*% v/v*)			
5.0	8.0	2.0	1127	0.9251	0.000389
5.0	7.0	4.0	1234	0.9214	0.000455
5.0	6.0	6.0	1397	0.9185	0.000503
5.0	5.0	8.0	1548	0.9173	0.000456
5.0	4.0	10.0	1741	0.9140	0.000455
5.0	3.0	12.0	1954	0.9116	0.000507
5.0	2.0	14.0	2241	0.9082	0.000528
5.0	1.0	16.0	2465	0.9067	0.000463

According to Table 4-4, the *Rs* value increases with the rising of ethanol concentration and reduce of the malic acid concentration. The linear correlation (Eq.4-7) shows an R^2 of 0.9822.

$$C_E = 0.01014Rs - 8.3798 \quad (4\text{-}7)$$

As illustrated in Chapter 3, the malic acid concentration has a power correlation with the solution resistance, which has an exponent of -2. However, compared with the linear correlation between the solution resistance and the ethanol concentration, the influence of malic acid decrease is much smaller. Hence, the correlation between ethanol concentration and the *Rs* value of simulation of solutions close to a linear correlation. Practically, this result can be used to detect the ethanol level in the solutions when the organic acid is found.

4.4 Conclusion

The impedance properties of sugar-ethanol, organic acids, tartaric acid-ethanol, and organic acids-ethanol compound solutions are investigated based on the findings of pure solutions.

A series of sugar-ethanol solutions with the concentrations simulating the real condition is analysed. Samples with descending sugar contents and ascending ethanol concentrations are tested. As a result, the impedance magnitude and diameter of Nyquist plot show a clear indication of the fermentation termination. The impedance magnitude and diameter of Nyquist semicircle are quite stable when the ethanol concentration is lower than 6%v/v. With the decreasing of sugar content, the impedance magnitude and diameter of Nyquist plot increase extremely. This phenomenon suggests that the *EIS* can be used to indicate the fermentation termination.

The *Rs-CPE* serial model is used to simulate the solution in an electrical cell for organic acids, tartaric acid-ethanol, and organic acids-ethanol compound solutions. In malic acid and tartaric acid mixed solutions, the *Rs* value shows a power correlation with the acid concentration similar as that of the pure solutions. As the tartaric acid concentration is relatively stable during the fermentation, a tartaric acid factor δ is introduced to adjust the correlation between the *Rs* and the malic acid concentration. The high R^2 (0.9798) of the fitting results confirms the veracity for malic acid measurement.

In tartaric acid-ethanol solutions, a linear correlation between ethanol concentration and the *Rs* value is found. As ethanol weakens the ionization of tartaric acid, the amount of free ions in the solutions is decreased, which leads to the increase of solution resistance. This linear relationship which has an R^2 of 0.9968 provides a deeper understanding of how ethanol influences the acid ionization and solution resistance.

Based on the results gained from binary solutions impedance tests, the solution which simulated the real fermentation condition with different concentration of malic acid, ethanol, and constant concentration of tartaric acid is investigated. As

a result, a linear relationship between ethanol content and *Rs* value is discovered. The research in tartaric acid and malic acid mixture shows a power correlation between malic acid concentration and the solution resistance. However, the ethanol- tartaric acid test suggests a stronger influence of acid ionization than of organic acids to each other. That means, the ethanol concentration is the most important factor which alter the solution resistance. Thus, it is possible to measure the wine ethanol content by *EIS* method as ethanol, tartaric acid and malic acid are the main components in wine.

Chapter 5
Validation Tests and Discussion

5.1 Validation Tests

As illustrated in previous chapters, research on pure solutions and compound solutions has been carried out. The tested samples include pure solutions, such as ethanol, malic acid and tartaric acid, and compound solutions, such as sugar-ethanol, malic-tartaric acid and ethanol-malic-tartaric solutions. As a result, linear and power relationships between solvent concentrations and impedance parameters, including impedance magnitude on specific frequency, diameter of the Nyquist semi-circle, and *Rs* value of the equivalent electrical circuit model, are found. Because one major aim of this research is to discuss the application of the *EIS* method in wine components measurement, the validation tests of the established model in this research are needed.

There are two parts to the validation tests that have been performed in this research. The first test is the ethanol concentration measurement in its pure solution, which is implemented for validating and comparing the precision of three *EIS* data analysis methods. The second test is the ethanol concentration measurement in real fermenting grape juice. As in previous experiments, all of these tests are duplicated three times. The measurements are based on the results of ethanol-malic-tartaric acid experiments in chapter 4.

5.1.1 Validation Test on Ethanol Pure Solution

As described in chapter 3, reactance on specific frequency and the diameter of the Nyquist semi-circle are two of the most precise analytical methods for *EIS* measurements, as the R^2 of them are 0.9668 for reactance and 0.9796 for the diameter of Nyquist semicircle. These two analytical methods are compared in the validation test.

Six ethanol solution samples, whose concentrations are unknown, are tested with the standard curve. These six samples which were prepared with specific concentrations were shuffled after numbers had been labeled.

Table 5-1 The result of validation test on ethanol pure solution. The concentrations calculated by reactance and diameter of Nyquist circle are listed.

No.	Concentration of Solutions	Z'' (Ω)	Concentration calculated by Z''	Error	Diameter (Ω)	Concentration Calculated by Diameter	Error
1	15.00%	1783367	16.04%	1.04%	3622367	14.85%	-0.15%
2	5.00%	1064600	5.03%	0.03%	2255100	4.43%	-0.57%
3	20.00%	1948533	18.57%	-1.43%	4279333	19.85%	-0.15%
4	30.00%	2642833	29.20%	-0.80%	5504533	29.19%	-0.81%
5	10.00%	1425267	10.55%	0.55%	2989867	10.03%	0.03%
6	25.00%	2425100	25.86%	0.86%	4911100	24.66%	-0.34%

As can be seen in Table 5-1, the errors of the concentration are less then 2%*v/v* in reactance of a single frequency, and the errors are less than 1%*v/v* when the diameters of Nyquist semi-circle are calculated. The reason why the diameter method is more accurate than the reactance method is that the diameter is the property of the whole Nyquist plot. Though a single spot on the Nyquist plot can be used as a characteristic value to assess the concentration, it is better to use all the spots on the Nyquist plot to measure the better result.

5.1.2 Validation Test on Real Grape Juice Fermentation

Wine fermentation is a complicated process as a series of physical changes and chemical reactions happen during the fermentation. In order to validate the effect of the *EIS* method applied on real wine analysis, a validation test on real grape fermentation is carried out.

The fermenting grape juice was taken from the fermentation tank of a local winery (Mount Moliagul Wines) during the harvest season of 2009. The fermentation period took 6 days. The grape juice samples were taken at 10 o'clock every morning during the fermentation process. Fermenting grape juice samples were deposited to remove the yeast then frozen after sampling, and kept frozen during transport in order to keep the grape juice fresh and minimize the evaporation of ethanol. The grape juice was defrosted back to room temperature before *EIS* measurements.

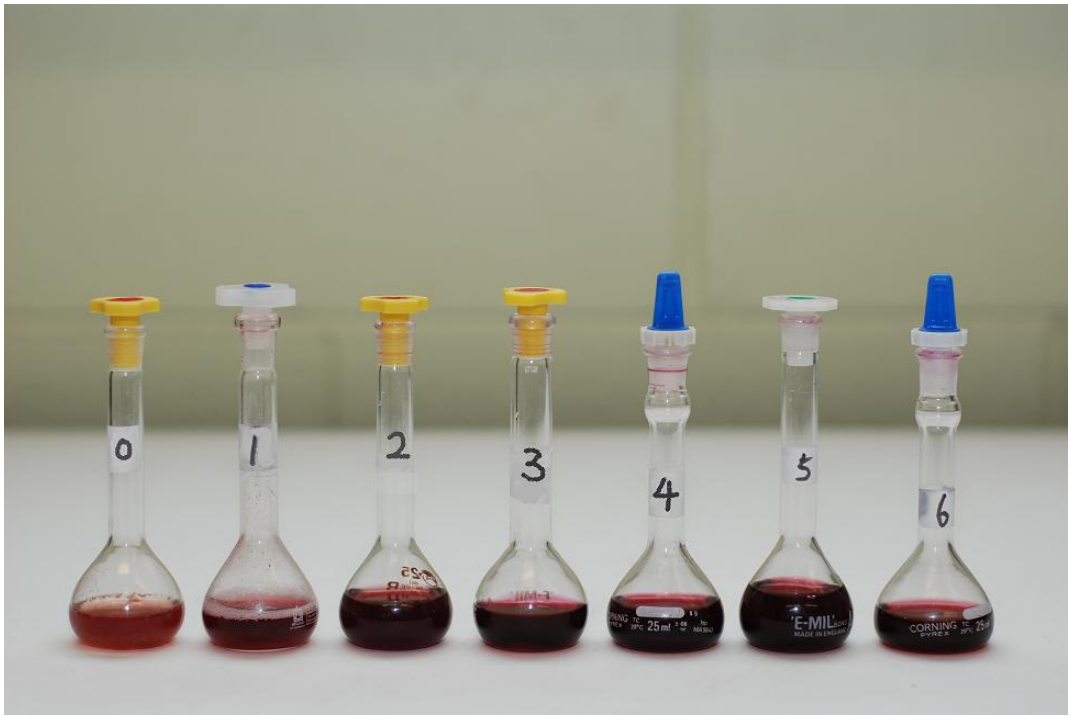

Figure 5-1 The grape juice samples taken from local winery. The volumetric flasks are labeled with the fermentation days of the wine. The No.0 sample was taken shortly after the yeast addition.

Figure 5-1 shows the grape juice samples taken from the winery. It can be seen clearly that the color of the grape juice samples changed gradually during the first 3 days. The fermentation became strong from day 1 to day 4.

The samples were also sent to measure the ethanol content by *GC* as a standard routine. *GC* is a well-known and widely used tool for ethanol concentration

measurement in wine industry. The principles and the complicated operating procedures of determining fermenting grape juice ethanol concentration is explained in Appendix A. The ethanol content finally stopped at 11.0%*v/v* at the end of fermentation. Figure 5-2 shows the ethanol concentration change during the whole fermentation time obtained by *GC*.

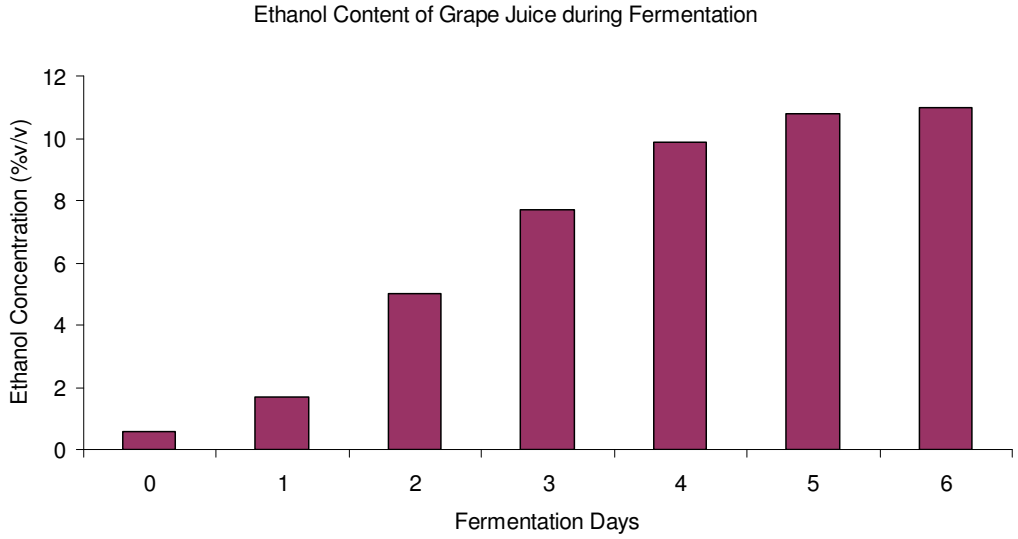

Figure 5-2 The ethanol concentration change during the fermentation period obtained by GC.

The ethanol concentration gain from *GC* and fitting results of the resistor-*CPE* serial model are listed in the Table 5-2. As can be seen, the *Rs* value has a decreasing trend when the ethanol concentration is increasing. However, both of the *CPE-T* and *CPE-P* values seem random as no clear correlation can be seen.

Table 5-2 The results of ethanol concentration measurement by *GC* and *EIS* methods.

Days	Ethanol Concentration by *GC (%v/v)*	*Rs (Ω)*	*CPE-T*	*CPE-P*	*Chi-Square*
0	0.6	588.46	4.89×10^{-5}	0.859584	0.000266
1	1.7	795.4	2.46×10^{-5}	0.904002	0.000243
2	5	798.84	3.00×10^{-5}	0.880052	0.000201
3	7.7	853	3.34×10^{-5}	0.88716	0.000287
4	9.9	885.48	2.22×10^{-5}	0.90954	0.000204
5	10.8	974.9	2.51×10^{-5}	0.90362	0.000315
6	11	1023.4	2.86×10^{-5}	0.881164	0.000261

The correlation between the concentration and *Rs* is fitted. The fitting result is shown in Figure 5-3. The Fitting formula (5-1) is similar to the result of malic acid, tartaric acid and ethanol compound solution in section 4.3.3.2, while the R^2 is 08216, which is relatively low.

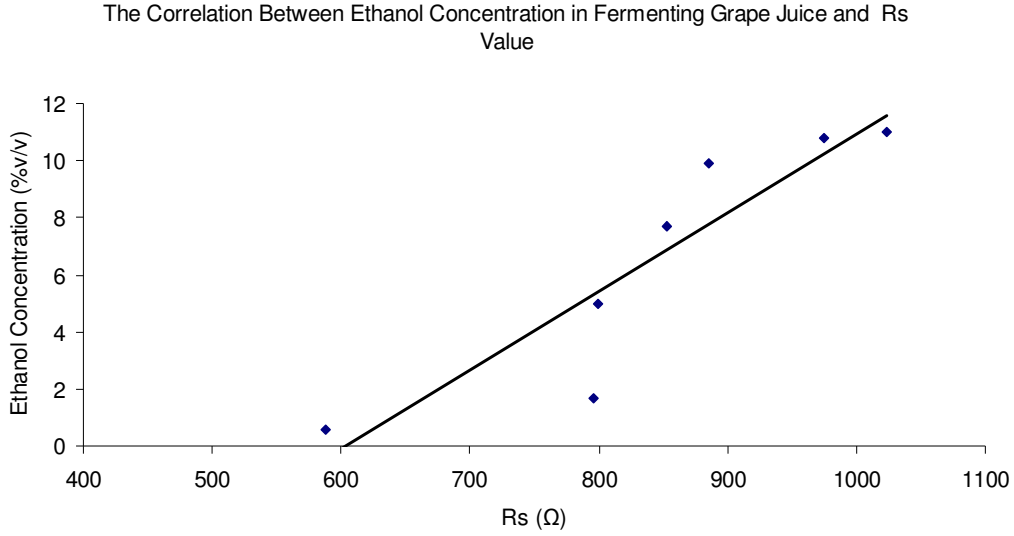

Figure 5-3 The correlation between ethanol concentration in fermenting grape juice and Rs value.

$$C_E = 0.0276Rs - 16.63 \quad (5\text{-}1)$$

The difference of coefficients between equation 4-7 and 5-1 is caused by a higher acidity and electrolyte concentration in grape juice than the malic acid, tartaric acid and ethanol compound solution. As grape juice contains metal ions, the conductivity is higher than the organic acid and ethanol compound solutions. However, the R^2 is relatively low, which may be caused by the following problems. The small carbon dioxide bubbles produced by yeast influence the performance of electrodes severely. The grape flesh which is normally present in grape juice is also a reason why the result has low precision. As these problems influence the precision of *EIS* measurements, future work is necessary to improve the electrode performance in practical applications.

5.2 Discussion

In the last hundred years, winemaking has benefitted from the industrial revolution and the development of science. People are always interested in the involved process when the grape must is made into wine and how to control it. Over the same period, the developments of chemistry and biology have greatly assisted wine science. Nowadays, fermentation control technologies based on wine science have greatly increased the production quantity of wine all over the world. At the same time, the wine quality is also improved as the fermentation control technologies have reduced the chance of fermentation failure. However, this is far from the end of technology development. Winemakers still need to wait at least one day to get the ethanol content measurement. That means if the fermentation went wrong, winemakers will receive the information when it is too late. Furthermore, professional devices like *HPLC* and *GC* limit the spreading of these tools. Most of the wineries are far from big cities where chemical labs with professional operators who can handle such wine analysis are located. The long distance transport of wine samples not only wastes time and money, but also increases the chance of sample loss and damage. That's the reason why a handy device, which can measure ethanol concentration and other important parameters immediately, is so important.

With the above motivation, this research investigates the feasibility of using the *EIS* method to measure the ethanol concentration in fermenting grape juice. As wine fermentation is a process with many complex physical changes and chemical reactions, this work begins with the measurement of pure solutions. Ethanol, tartaric acid and malic acid which are three of the most important components in wine are tested. Then, based on the discovery of the relationships between impedance parameters (especially the diameter of the Nyquist semicircle in ethanol solutions and the solution resistances in organic acid solutions) and solvent concentrations, compound solutions are researched. Following the analysis of ethanol solutions, a mixture of ethanol and sugar solution is researched. Similarly, the compound solution of tartaric acid and malic acid is tested by *EIS* and analysed. These experiments and analysis build a foundation of the *EIS* method for wine analysis. Then, the solution with tartaric acid, malic acid and

ethanol are investigated. The result of three-component-solutions shows a clear linear relationship between ethanol concentration and solution resistance. Basically, the resistance of an organic acid solution, which is highly related to the free ions content, is a response of the ionization ability of the organic acid. The ethanol in solutions not only increases the imaginary part (reactance) of solution impedance, but also weakens the ionization of organic acid. The experiments also confirmed the theoretical deductions, which explain that the extent for ionization variation is highly related to the ethanol concentration. These findings suggest a bright future of *EIS* method in wine analytical applications.

As the *EIS* method of wine analysis is still at an early stage, problems still exist. One is that this method relies on measuring the ionization variation of organic acids in wine to indicate the ethanol concentration. Though the organic acid concentration does not influence the ethanol measurement much, it could reduce the precision of the ethanol measurement if it changes significantly in some cases. And practically, yeast produces numerous of carbon dioxide bubbles during the wine fermentation. These little bubbles can easily influence the electrodes and greatly increase the impedance value. When the real fermentation samples are tested, the yeast removal and freezing procedures reduce the carbon dioxide bubbles. However, some bubbles are still there though they are very small and almost invisible. Thus, it is necessary to reduce the influence of carbon dioxide bubbles.

Naturally, before solving these problems, the *EIS* method still cannot replace the traditional tools like *HPLC* and *GC*, etc. These traditional methods, which scientists all over the world have contributed their effort to, have developed over many years. Compared with *EIS*, they still have many advantages such as very high precision and reliability. However, their disadvantages, such as high cost, slow measurement and the need for professional operators limit their application. By using microchip technology, it is easy to design a light-weight and low-cost impedance analyzer which is easy to operate. As the *EIS* signal is collected by computer, it is possible to setup a computer program to control the wine fermentation environment according to the *EIS* measurement automatically. The self-monitoring system based on the *EIS* method may save labour and reduce production costs.

Figure 5-4 illustrates a possible self-monitoring system in the future. The impedance analyzer generates *EIS* via electrodes which are attached to the inner wall of the fermentation tank. A Multi-channel Switch is used to switch the impedance analyzer connected to each fermentation tank when there is more than one tank working. The monitoring computer collects and analyses the impedance data, then the test results can be transmitted to a portable monitoring device via wireless, or the fermentation environment controller, which can adjust the temperature, acidity, oxygen and other fermentation conditions by *EIS* results.

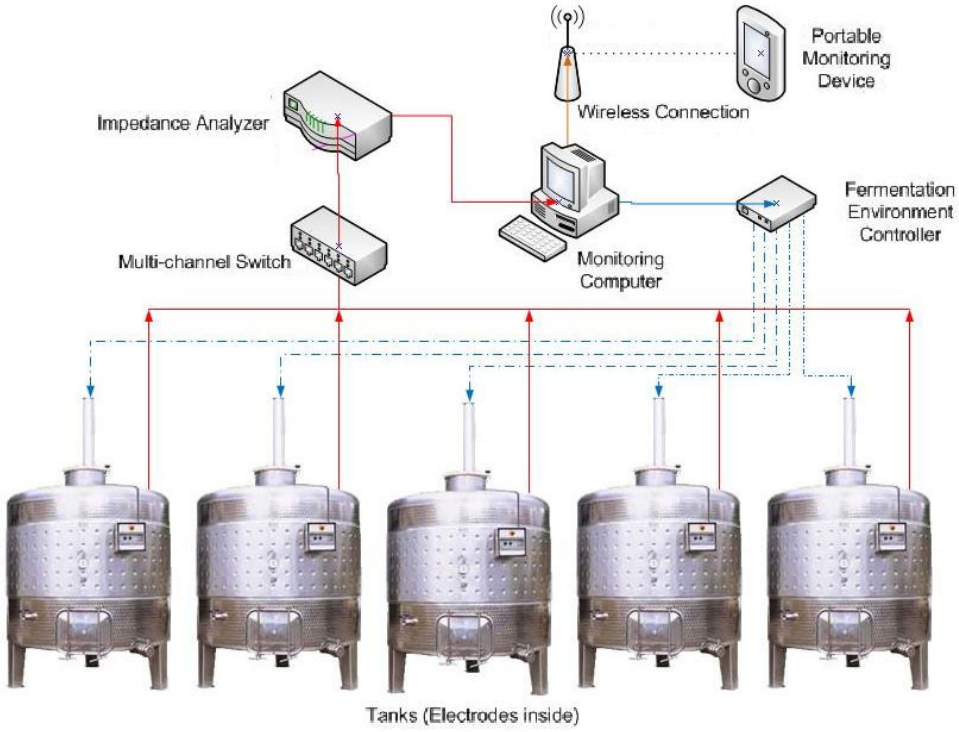

Figure 5-4 An outline of fermentation automated system based on EIS method.

Portable impedance analyzer will also be available for small wineries. The winemaker will just need to insert the electrodes into fermenting grape juice, then the ethanol concentration will display on the *LCD* screen in minutes.

Chapter 6
Conclusions and Future Research

6.1 Conclusions

An investigation into the electrical properties of major constituents of fermenting grape must by *EIS* is presented in this thesis. A set of linear and power correlations are found by experiments and related theoretical deductions on pure solutions and compound solutions of these major constituents. Following is the conclusion of these findings.

The electrical impedance properties of pure ethanol solution are investigated. There are three data analysis methods used to measure impedance of these solutions. With a single frequency spectroscopy, impedance magnitude and reactance both show good correlation with the ethanol concentration, where the R^2 is 0.9160 for impedance magnitude, and 0.9668 for reactance. On the other hand, the diameter of the Nyquist semicircle shows better correlation (the R^2 is 0.9796) with the ethanol concentration. Thirdly, an equivalent electrical model is also used to simulate the distributed transmission of electrons in solution. Fitted with the resistor-*CPE* parallel model, the *Rs* value has strong linear correlation with solution concentration with an R^2 of 0.9733 while there is only a moderate correlation between *CPE-P* and concentration with an R^2 of determination of 0.8124.

The malic acid and tartaric acid pure solutions are investigated. Oblique line shaped Nyquist plots are shown by *EIS* measurements in these solutions. A model which consists of a resistor and a serial *CPE* is designed to remove electrode impedance and polarization impedance in organic acid solutions. The tests of the pure solutions of organic acids and following compound solutions with organic acids and ethanol confirm the efficiency of the model. By theoretical deduction and experiments, a power correlation between *Rs* value and the acid concentration is found. The correlation which has high R^2 values (0.9977 for tartaric acid and

0.9887 for malic acid) suggests the high precision for organic acid concentration determination by this *EIS* based method.

The sugar-ethanol compound solutions are made to simulate the real conditions of ethanol fermentation. The impedance magnitude and reactance on specific frequency are also discussed. They change little when the ethanol concentration is lower than 6%. However, when the ethanol concentration is higher than 6%, a great rise of impedance magnitude and reactance on specific frequency occurs. The diameter of the Nyquist semicircle has the same trend as the impedance magnitude and reactance, while the diameter change with concentration looks smoother than that of impedance magnitude and reactance. These findings suggest that the fermentation end point can be indicated by a significant increase in the impedance parameters discussed above.

A series of compound solutions with stable concentrations of tartaric acid and variable concentrations of malic acid, which is similar to the conditions of real wine fermentation, are tested by *EIS*. The *Rs* value generated by using the resistor-*CPE* serial model shows a power relationship with the malic acid concentration. The high R^2 value (0.9798) shows that *EIS* is an efficient method to measure the malic acid concentration.

Based on the discoveries mentioned above, the tartaric acid and ethanol compound solution is tested to investigate the influence of ethanol concentration to the ionization of tartaric acid. The resistor-*CPE* serial model is used. As a result, a strong linear relationship between ethanol concentration and Rs value of the compound solution is found. The linear correlation has a high R^2 of 0.9968, which confirms that the ethanol in the solution weakens the ionization of tartaric acid linearly. This finding suggests the ethanol concentration in wine can be measured by using resistor-*CPE* serial model.

Using the same resistor-*CPE* serial model, the compound solution consisting of malic acid, tartaric acid and ethanol with concentrations similar to real wine fermentation is also tested. The malic acid concentration has power correlation with the *Rs* value, where the *Rs* value changes little when the malic acid

concentration changes. For this reason, ethanol concentration approximately has a linear correlation with the *Rs* value, which has an R^2 value of 0.9822.

Furthermore, validation tests on pure ethanol solution as well as real fermenting grape juice are carried out. The validation test on ethanol solution shows a good precision of 1%*v/v*. However, the real fermenting grape juice shows relatively low correlation with *Rs* value as the R^2 is 0.8216, though the formula is very close to that of compound solutions, which suggests that the carbon dioxide bubbles and grape flesh in the juice may influence the *EIS* precision. Removal of these influence factors could be a focus of future work.

6.2 Future Research

This thesis has explored the *EIS* method applied to wine ethanol and organic acids concentration measurement. The experiments on pure solutions and compound solutions provide a clear understanding of impedance performance of solutions, especially electrolyte solutions, which contains major constituents of fermenting grape must. However, as a complicated compound solution, grape must contains numerous electrolytes, ions, soluble nonelectrolyte (such as ethanol), and small amounts of protein, peptides and pigments, etc. This situation makes the development of a new method for quantitative analysis of wine very challenging.

Though this research established the *EIS* method of ethanol concentration measurement, the validation test on real fermenting grape juice is still not satisfactory. Carbon dioxide bubbles, electrodes stability, grape flesh and other remnants can influence the impedance measurement to reduce the precision. At this stage, it is difficult to improve the accuracy due to these existent disturbance factors. In the future work, sample pretreatment could be used to minimize or remove these disturbance factors. For example, the small carbon dioxide bubbles can be removed by ultrasound concussion, and the grape flesh can be removed by centrifuge or filtering. If these pretreatments can be applied inside the fermentation tank, *EIS* method could have the possibility for commercial use.

On the other hand, the Solartron frequency response analyzer used in this research is still an expensive and huge device. As discussed in Chapter 5, a practical device should be handy and easy to operate, also cheap. In validation tests, the measurement of ethanol concentrations in real fermenting grape juice only requires a frequency range of 1-100*Hz*, which suggests that the high frequency part of the frequency response analyzer can be removed. This would simplify the design of impedance analyzer and lower the cost.

In conclusion, the *EIS* method is worth researching and its potential in wine analysis is huge. Future research can focus on solving the problems demonstrated above, and improving the precision and design of the impedance analyzer. *EIS* methods research may also be appropriate for other alcoholic beverages, such as beer and cocktails.

References

[1] FSANZ, "Australia-only Standard 4.1.1 - Wine Production Requirements." vol. 1, Food Standards Australia New Zealand, Ed.: FSANZ, 2002.

[2] Australian Bureau of Statistics, *Australian Wine and Grape Industry*: Australian Bureau of Statistics, 2007.

[3] FAO, "The World Agriculture Production," Food and Agriculture Organization of the United Nations, Ed.: FAOSTAT, 2007.

[4] M. Van Sint Jan, M. Guarini, A. Guesalaga, J. R. Perez-Correa, and Y. Vargas, "Ultrasound Based Measurements of Sugar and Ethanol Concentrations in Hydroalcoholic Solutions," *Food Control,* vol. 19, pp. 31-35, 2008.

[5] V. V. Meriakri and E. E. Chigrai, "Determination of Alcohol and Sugar Content in Water Solutions by Means of Microwave," in *MSMW' 04 Symposium* Kharkov, Ukraine: IEEE, 2004.

[6] T. Repo, "The Electrical Impedance of Plant Tissues," in *International Conference on Electrical Bioimpedance and Electrical Impedance Tomography*, Poland, 2004, pp. 37-40.

[7] M. A. Cox, M. I. N. Zhang, and J. H. M. Willison, "Apple Bruise Assessment Through Electrical Impedance Measurements," *Journal of Horticultural Science,* vol. 68, pp. 393-398, 1993.

[8] F. R. Harker and S. K. Forbes, "Ripening and Development of Chilling Injury in Persimmon Fruit: an Electrical Impedance Study," *New Zealand Journal of Crop and Horticultual Science,* vol. 25, pp. 149-157, 1997.

[9] S. Zougar, K. Morakchi, A. Zazoua, S. Saad, R. Kherrat, and N. Haffrezic-Renault, "Characterization of ammonium ion - Sensitive membranes in solution with electrochemical impedance spectroscopy," *Material Science and Engineering C,* vol. 28, pp. 1020-1023, 2008.

[10] F. Kuralay, A. Erdem, S. Abaci, H. Ozyoruk, and A. Yildiz, "Characterization of redox polymer based electrode and electrochemical behavior for DNA detection," *Analytica Chimica Acta,* vol. 643, pp. 83-89, 2009.

[11] S. Cho and H. Thielecke, "Electrical characterization of human mesenchymal stem cell growth on microelectrode," *Microelectronic Engineering,* vol. 85, pp. 1272-1274, 2008.

[12] M. G. Silva, S. Helali, C. Esseghaier, C. E. Suarez, A. Oliva, and A. Abdelghani, "An impedance spectroscopy method for detection and evaluation of Babesia bovis antibodies in cattle," *Sensors and Actuators B,* vol. 135, pp. 206-213, 2008.

[13] R. B. Boulton, V. L. Singleton, L. F. Bisson, and R. E. Kunkee, *Principles and Practices of Winemaking*. Gaithersburg, Maryland: Aspen Publishers, Inc., 1998.

[14] J. Goode, *The Science of Wine*. London: Octopus Publishing Group Ltd, 2005.

[15] K. S. Cole and H. J. Curtis, "Bioelectricity: Electric Physiology," in *Medical Physics*. vol. 2, O. Glasser, Ed. Chicago: the Year Book Publisher INC., 1950, pp. 82-90.

[16] C. K. Alexander and M. N. O. Sadiku, *Fundamentals of Electric Circuits*, 2nd ed. Boston, New York, San Francisco: McGraw-Hill, 2004.

[17] B. W. Zoecklein, K. C. Fugelsang, B. H. Gump, and F. S. Nury, *Wine Analysis and Production*. New York: Chapman & Hall, 1995.

[18] L. M. L. Nollet, *Food Analysis by HPLC*, 2nd ed. New York: Marcel Dekker, Inc., 2000.

[19] S. J. Haswell, *Atomic Absorption Spectrometry: Theory, Design and Applications* vol. 5. Amsterdam: Elsevier Science Publishers B.V., 1991.

[20] S. S. Nielsen, *Food Analysis*, 2nd ed. Gaithersberg: Aspen Publishers, Inc., 1998.

[21] M. McMaster, *GC/MS: A Pratical User's Guide*, 2nd ed. Hoboken: John Wiley & Sons, Inc., 2008.

[22] Y. Ozaki, M. W.F., and A. A. Christy, *Near-Infrared Spectroscopy in Food Science and Technology*. Hoboken: John Wiley & Sons, Inc., 2007.

[23] J. Matthie, B. Zarowitz, A. De Lorenzo, A. Andreoli, K. Katzarski, G. Pan, and P. Withers, "Analytic Assessment of the Various Bioimpedance Methods Used to Estimate Body Water," *The American Physiological Society,* pp. 1801-1816, 1998.

[24] C. M. Thompson, C. H. Kong, C. A. Lewist, P. D. Hill, and F. D. Thompson, "Can Bio-electrical Impedance Be Used to Measure Total Body Water in Dialysis Patients?," *Physiol. Meas.,* vol. 14, pp. 455-461, 1993.

[25] A. De Lorenzo and A. Andreoli, "Segmental Bioelectrical Impedance Analysis," *Curr Opin Clin Nutr Metab Care,* vol. 6, pp. 551-555, 2003.

[26] R. Patterson, "Body Fluid Determinations Using Multiple Impedance Measurements," *IEEE Engineering in Medicine and Biology Magazine,* vol. 8, pp. 16-18, 1989.

[27] U. G. Kyle, I. Bosaeus, A. D. De Lorenzo, P. Deurenberg, M. Elia, J. M. Gomez, B. L. Heitmann, L. Kent-Smith, J. Melchior, M. Pirlich, H. Scharfetter, A. M. W. J. Schols, and C. Pochard, "Bioelectrical Impedance Anlysis-part I: Review of Principles and Methods," *Clinical Nutrition,* vol. 23, pp. 1226-1243, 2004.

[28] D. A. Schoeller, "Bioelectrical Impedance Analysis: What Does it Measure?," *Annals of the New York Academy of Sciences,* vol. 904, pp. 159-162, 2000.

[29] A. P. Hills and N. M. Byrne, "Bioelectrical Impedance and Body Composition Assessment," *Mal. J. Nutr.,* vol. 4, pp. 107-112, 1998.

[30] E. M. Lehnert, D. D. Clarke, J. G. Gibbons, L. C. Ward, S. M. Golding, R. W. Shepherd, B. H. Cornish, and D. H. G. Crawford, "Estimation of Body Water

Compartments in Cirrhosis by Multiple-Frequency Bioelectrical Impedance Analysis," *Nutrition,* vol. 17, pp. 31-34, 2001.

[31] P. Deurenberg, A. Andreoli, and A. De Lorenzo, "Multi-frequency Bioelectrical Impedance:a Comparison between the Cole-Cole Modeling and Hanai Equations with the Classical Impedance Index Approach," *Ann. Hum. Biol.,* vol. 6, pp. 31-40, 1996.

[32] U. G. Kyle, I. Bosaeus, A. D. De Lorenzo, P. Deurenberg, M. Elia, J. M. Gomez, B. L. Heitmann, L. Kent-Smith, J. Melchior, M. Pirlich, H. Scharfetter, A. M. W. J. Schols, and C. Pochard, "Bioelectrical Impedance Analysis-part ii:Utilization in Clinical Practice," *Clinical Nutrition,* vol. 23, pp. 1430-1453, 2004.

[33] T. Repo, G. Zhang, A. Ryyppo, and R. Rikala, "The Electrical Impedance Spectroscopy of Scots Pine (*Pinus Sylvestris L.*) Shoots in Relation to Cold Acclimation," *Journal of Experimental Botany,* vol. 51, pp. 2095-2107, 2000.

[34] J. R. MacDonald, "Impedance Spectroscopy," *Annals of Biomedical Engineering,* vol. 20, pp. 289-305, 1992.

[35] J. R. MacDonald and L. D. Potter, "A Flexible Procedure for Analyzing Impedance Spectroscopy Results:Description and Illustrations," *Solid State Ionics,* vol. 23, pp. 61-79, 1987.

[36] H. G. Goovaerts, T. J. C. Faes, G. W. de Valk-de Roo, M. ten Bolscher, J. C. Netelenbosch, W. J. F. van der Vijgh, and R. M. Heethaar, "Extra-cellular Volume Estimation by Electrical Impedance-Phase Measurement or Curve Fitting: A Comparative Study," *Physiol. Meas.,* vol. 19, pp. 517-526, 1998.

[37] A. D. Bauchot, F. R. Harker, and W. M. Arnold, "The Use of Electrical Impedance Spectroscopy to Assess the Physiological Condition of Kiwifruit," *Postharvest Biology and Technology,* vol. 18, pp. 9-18, 2000.

[38] J. J. Ackmann and M. A. Seitz, "Methods of Complex Impedance Measurements in Biological Tissues," *CRC Crit. Rev. Biomed. Eng.,* vol. 11, pp. 281-311, 1984.

[39] F. R. Harker and J. Dunlop, "Electrical Impedance Studies of Nectraines During Coolstage and Fruit Ripening," *Postharvest Biology and Technology,* vol. 4, pp. 125-134, 1994.

[40] C. D. Ferris, *Introduction to Bioelectrodes*. New York: Plenum Press, 1974.

[41] H. P. Schwan, "Determination of Biological Impedances," in *Physical Techniques in Biological Research*. vol. 323, W. L. Nastuk, Ed. New York: Academic Press, 1963.

[42] M. I. N. Zhang and J. H. M. Willison, "Electrical Impedance Analysis in Plant Tissues: A Double Shell Model," *Journal of Experimental Botany,* vol. 42, pp. 1465-1475, 1991.

[43] T. Shedlovsky, *J. Am. Chem. Soc.,* vol. 52, p. 1806, 1930.

[44] C. Glerum, "Annual Trends in Frost Hardiness and Electrical Impedance for Seven Coniferous Species," *Can. J. Plant Sci.,* vol. 53, pp. 881-889, 1973.

[45] T. Repo, "Seasonal Changes of Frost Hardiness in *Pices abies* (L.) Karst. and *Pinus sylvestris* (L.) in Finland," *Can. J. Forest Res.,* vol. 22, pp. 1949-1957, 1992.

[46] K. H. Freywald, F. Pliquett, L. Schoberlein, and U. Pliquett, "Passive Electrical Properties of Meat as a Characteristic of its Quality," in *the IX. International Conference on Electrical Bio-impedance*, Heidelberg, Germany, 1995, pp. 366-369.

[47] M. E. Orazem and T. Bernard, *Electrochemical Impedance Spectroscopy*. Hoboken: John Wiley & Sons, Inc., 2008.

[48] A. R. Varlan and W. Sansen, "Nondestructive Electrical Impedance Analysis in Fruit: Normal Ripening and Injuries Characterization," *Electro- and Magnetobiology,* vol. 15, pp. 213-227, 1996.

[49] J. R. MacDonald and J. A. Garber, "Analysis of Impedance and Admittance Data for Solids and Liquds," *Journal of the Electrochemical Society,* vol. 124, pp. 1022-1030, 1977.

[50] G. Otto, "Bioelectricity: Electric Physiology," in *Medical Physics Year Book*. vol. 2, K. S. Cole and H. J. Curtis, Eds. Chicago: The Year Book Publishers, 1950, pp. 82-90.

[51] R. I. Hayden, C. A. Moyse, F. W. Calder, D. P. Carwford, and D. S. Fensom, "Electrical Impedance Studies on Potato and Alfalfa Tissue," *Journal of Experimental Botany,* vol. 20, pp. 177-200, 1969.

[52] F. R. Harker and J. H. Maindonald, "Ripening of Nectarine Fruit," *Plant Physiol.,* vol. 106, pp. 165-171, 1994.

[53] M. I. N. Zhang and J. H. M. Willison, "Electrical Impedance Analysis in Plant Tissues: Impedance Measurement in Leaves," *Journal of Experimental Botany,* vol. 44, pp. 1369-1375, 1993.

[54] J. B. Jorcin, M. E. Orazem, N. Pebere, and B. Tribollet, "CPE Analysis by Local Electrochemical Impedance Spectroscopy," *Electrochimica Acta,* vol. 51, pp. 1473-1479, 2006.

[55] A. Lasia, Electrochemical Impedance Spectroscopy and its Applications in Modern Aspects of Electrochemistry vol. 32. New York: Kluwer Academic/Plenum Publishers, 1999.

[56] P. Zoltowski, "On the electrical capacitance of interfaces exhibiting constant phase element behaviour," *Electroanalytical Chemistry,* vol. 443, pp. 149-154, 1998.

[57] C. Gabrielli, "Use and Applications of Electrochemical Impedance Techniques," England, Schlumberger Technical Report 1993.

[58] B. H. Cornish, B. J. Thomas, and L. C. Ward, "Improved Prediction of Extracellular and Total Body Water Using Impedance Loci Generated by Multiple

Frequency Bioelectrical Impedance Analysis," *Phys. Med. Biol.,* vol. 38, pp. 337-346, 1993.

[59] R. E. Kirk, *Statistics, An Introduction*, 4th ed. Orlando, USA: Holt, Rinehart and Winston, USA, 1999.

[60] N. R. Draper, *Applied Regression Analysis*, 3rd ed. New York: Wiley, 1998.

[61] A. R. Varlan and W. Sansen, "Multifrequency Impedance Measurement for Fruit Quality Evaluation," *Innovation and Technology in Biology and Medicine,* vol. 16, pp. 727-735, 1995.

[62] X. Liu, "Electrical Impedance Spectroscopy Applied in Plant Physiology Studies," in *School of Electrical and Computer Engineering* Melbourne, Australia: RMIT University, 2006, p. 102.

[63] R. J. Furmanski and R. W. Buescher, "Influence of Chilling on Electrolyte Leakage and Internal Conducitivity of Peach Fruits," *HortScience,* vol. 14, pp. 167-168, 1979.

[64] M. I. N. Zhang, D. G. Stout, and J. H. M. Willison, "Electrical Impedance Analysis in Plant Tissue: Symplastic Resistance and Membrane Capacitance In the Hayden Model," *J. Exp. Bot.,* vol. 41, pp. 371-380, 1990.

[65] T. Repo, "Influence of Different Electrodes and Tissues on the Impedance Spectra of Scots Pine Shoots," *Electro- and Magnetobiology,* vol. 13, pp. 1-14, 1994.

[66] J. M. Labavitch, L. C. Greve, and E. Mitcham, "Fruit Bruising: It's More than Skin Deep," in *Perishables Handling Quarterly Issue*, 1998, pp. 7-9.

[67] S. Gunasekaran, Nondestructive Food Evaluation: Techniques to Analyze Properties and Quality. New York: MerceL Dekker, Inc., 2001.

[68] E. Vozary, P. Laszlo, and G. Zsivanovits, "Impedance Parameter Characterizing Apple Bruise," *Annals New York Academy of Sciences,* vol. 873, pp. 421-429, 1999.

[69] P. J. Jackson and F. R. Harker, "Apple Bruise Detection by Electrical Impedance Measurement," *HortScience,* vol. 35, pp. 104-107, 2000.

[70] S. Lurie and C. H. Crisosto, "Chilling Injury in Peach and Nectarine," *Postharvest Biology and Technology,* vol. 37, pp. 195-208, 2005.

[71] M. E. Saltveit, "The Rate of Ion Leakage from Chilling-Sensitive Tissue Does Not Immediately Increase upon Exposure to Chilling Temperatures," *Post. Biol. Technol.,* vol. 26, pp. 295-304, 2002.

[72] T. Fukushima and M. Yamazaki, "Chilling-Injury in Cucumbers. V. Polysaccharide Changes in Cell Walls," *Scientia Horticulturae,* vol. 8, pp. 219-227, 1978.

[73] J. Niu and J. Y. Lee, "A New Approach for the Determination of Fish Freshness by Electrochemical Impedance Spectroscopy," *Journal of Food Science,* vol. 65, pp. 780-785, 2000.

[74] D. L. Marshall and P. L. Wiese-Lehigh, "Comparison of Impedance, Microbial, Sensory, and pH Methods to Determine Shrimp Quality," *J. Aquatic Food Product Technology,* vol. 6, pp. 17-31, 1997.

[75] T. Stevenson, *The New Sotheby's Wine Encyclopedia*, 3rd ed. New York: DK Publisher, 2001.

[76] F. Dion and A. Lasia, "The use of regularization methods in the deconvolution of underlying distributions in electrochemical processes," *Electroanalytical Chemistry,* vol. 475, pp. 28-37, 1999.

[77] P. Atkins and J. D. Paula, *Physical Chemistry*. Oxford: Oxford University Press, 2006.

[78] M. S. Rocha and J. R. Simoes-Moreira, "A Simple Impedance Method for Determination Ethanol and Regular Gasoline Mixtures Mass Contents," *Fuel,* vol. 84, pp. 447-452, 2005.

[79] B. M. Grafov and B. B. Damaskin, "Theory of Electrochemical Faradiac Impedance for Mixed Electrolyte Solutions," *Electrochimica Acta,* vol. 41, pp. 2707-2714, 1996.

[80] G. T. Castro, O. S. Giordano, and S. E. Blanco, "Determination of the pKa of Hydroxy-benzophenones in Ethanol-water Mixtures and Solvent Effects," *Journal of Molecular Structure (Theochem),* vol. 626, pp. 167-178, 2003.

Appendix A
Background of Winemaking

A.1 Introduction

Winemaking has a long history which is as old as human civilization. Historically, winemakers improved winemaking procedures slowly by a combination of folklore, observation and luck. However, their failures monumentally stimulated the development of wine science and also caused some unanticipated results, such as vinegar. In modern times, the cost of grapes, physical and chemical technologies used in production, oak barrels, corks bottling equipment, etc., have increased dramatically and continue to rise. Though the major winemaking procedures have been established for thousands of years, the use of science to control winemaking has only developed over the past hundred years. Due to the development of wine science, consumers can now enjoy high-quality wine at low prices instead of expensive wines which were limited to aristocrats. In order to better understand how modern science can influence traditional winemaking, a brief review of it is provided in this section.

A.2 Winemaking Procedures

Winemaking is a very complicated process. It starts from the selection of the grapes or other produce, ending with bottling the finished wine. Two general categories are defined in winemaking, which are still wine production (without carbonation) and sparkling wine production (with carbonation). As main procedures of these two wine categories are similar, a brief overview of still wine production is given as an example.

A.2.1 Processing the Grape

Wine can be divided into three main species by colour. Red wine is made from the must of red or black grapes which are fermented with the grape skin, while white wine is usually made by fermenting juice pressed from white grapes. White wine can also be made from must extracted from red grapes without contacting grape skins. Rosé wines are made from red grapes where the juice is allowed to contact with the dark skins long enough to pick up a pinkish colour.

Wine grapes are picked after analysis of sugar content and acidity. The decision to harvest typically depends on Sugar *Brix*, Titratable Acidity and *pH* value of the grapes. Grapes are harvested by hand or mechanically. Crushing and destemming are two important processes before fermentation. The first one gently squeezes the grape berries to break the skins to liberate the content of them. It is carried out by a mechanical crusher in large wineries. Destemming process is also needed to remove most of the tannin which is mainly concentrated in the stems. The winemaker may decide to leave part of the stem to control the tannin quantity of wine. For white wine, the grapes are processed without destemming or crushing, just by pressing. After pressing, the skins of white grapes are removed. In the case of rosé wines, the dark berries are crushed follower by short contact with their skins to extract the color that the winemaker desires. The must is then pressed, and fermented as if the winemaker is making a white wine. The pressing procedure for red wine is done after fermentation.

A series of treatments is applied to grape juice and must in order to get ready for fermentation. First, sulfur dioxide is added to inhibit oxidizing enzymes, to inhibit

or kill most of the natural microorganism in the juice and must and to increase the acidity. Carbonate salts are added to reduce titratable acidity if the acidity is too high. Calcium carbonate can be used to neutralize the titratable acidity and to precipitate calcium tartrate, or mixtures of calcium tartrate and calcium malate. [13]

A.2.2 Primary Fermentation

The primary fermentation is also called ethanol fermentation, which is the most important step for ethanol producing by adding yeasts in grape juice. Two of the most commonly used yeasts for ethanol fermentation are *Saccharomyces cerevisiar* and *Saccharomyces bayanus*. During primary fermentation, the yeast cells feed on the sugars in the juice and must, producing carbon dioxide and ethanol. The temperature during the fermentation affects the fermentation speed and the quality of wine as carbon dioxide and ethanol are not the only products of yeasts. As the yeasts release heat during fermentation, temperature control is needed if the temperature increases too much. Wine yeast strains can be killed rapidly at a temperature over $42°C$. High temperature also leads to the production of undesirable byproducts of other microorganisms. For this reason, generally, the temperature of red wine fermentation is not permitted to rise above $30°C$, and that of white wine even lower. The termination of fermentation is indicated when most of the sugars have been consumed.

Yeast metabolism during fermentation is a complicated process. Ethanol is produced via the carbon metabolism conducted by a series of physiological cycles and pathways, such as *TCA* pathways, the pentose phosphate pathway and the glyoxylate cycle. The pentose phosphate pathway also produces plenty of aromatic amino acids which constitute the aroma of wine. The amount of ethanol produced by sugar during the wine fermentation can be approximately calculated by an expression which is defined by experience. Theoretically, 180g Sugar can be converted to $88g$ of carbon dioxide and $92g$ of ethanol. However, this is only expected when the yeast growth and ethanol evaporation is ignored. [13]

A.2.3 Clarification and Stabilization

After primary fermentation, a cold stabilizing process is carried out. During this process, the temperature of the wine is dropped close to freezing for 1-2 weeks. This procedure removes insoluble and suspended materials which may cause the wine to become cloudy and gassy. It precipitates unwanted sediment including tartrate crystals which is mainly potassium bitartrate.

A.2.4 Secondary fermentation and aging

As most sugar has been consumed by the yeast, secondary fermentation focuses on malolactic conversion. Three strains of lactic-acid bacteria react during malolactic fermentation: *Lactobacillus Oenococcus, Lactobacillus Leuconostoc, and Lactobacillus Pediococcus*. [14] This fermentation actually starts at the beginning of ethanol fermentation. Carried out by lactic-acid bacteria, this fermentation involves transforming malic acid into lactic acid. This procedure decreases the titratable acidity, increases the *pH* value and also changes the flavour of the wine. The fermentation continues slowly, taking three to six months. Proteins, remaining yeast cells and other insoluble particles are settled during this process. The visible result of secondary fermentation and aging is that the cloudy wine becomes clear. The sediment, which is called lees, can be filtered during these processes. The end products should be tested to check if the status of the wine meets the production standard. Common tests include *Brix*, *pH*, titratable acidity, residual sugar, free or available sulfur, total sulfur, volatile acidity and percentage of alcohol. [1] The wine products can then be bottled and sealed with a cork or screw cap.

A.3 The Future of Fermentation Control

Definitely, winemaking is a procedure for turning grape juice into an alcoholic beverage. It is no doubt that fermentation is the most important step. The product cannot be called "wine" until fermentation has finished. With the increasing consumption of wine all over the world, wine production is no longer a workshop style production, but an industrial procedure. In this situation, a fermentation management tool with a standardized monitoring system is necessary.

Fermentation control for industrial products always requires automation. During the fermentation period, many parameters need to be monitored and controlled, such as ethanol levels, acidity, sugar, etc. If these monitoring and controlling can be carried out automatically, not only the labour cost for winery maintenance can be saved, but also the quality of fermentation process can be guaranteed by reliable devices. Currently, analytical tools used in wine analysis include chemical techniques, High Performance Liquid Chromatography (*HPLC*), Atomic Absorption (*AAS*), Gas Chromatography (*GC*), Gas Chromatography / Mass Spectrometry (*GC-MS*), and Near Infrared Spectroscopy (*NIR*). They have advantages and disadvantages. Most of these technologies require expensive devices, which will affect the product cost. (More information about traditional analysis techniques is presented in Chapter 2.) These technologies cannot provide a real-time response which can deliver the result immediately. The slow response speed of traditional wine analytical techniques becomes a bottleneck in the development of monitoring and automated systems for wine fermentation. For this reason, a quick response method for wine analysis during the fermentation period is needed.

Appendix B
The Operating Procedures of GC for Wine Ethanol Determination

B.1 Principle of GC

Like any other chromatographic techniques, the movement of a sample through a gas chromatography (*GC*) column depends on the way it moves between the mobile and stationary phase. The mobile phase in GC is a gas (usually nitrogen or helium) that is passed continually through the apparatus. The stationary phase is a viscous liquid. The liquid sample is injected into the gas stream, where it is heated to vapor. The following gas stream then carries the sample into the column, where a portion of the sample will dissolve in the column liquid. So a section of the column now has column liquid containing the dissolved sample in contact with gas containing no sample. As the solution moves down the length of the column, the sample is transferred from the liquid to the gas and back again, slowing the samples passage. Different samples are slowed by different amounts so that when a sample containing a number of different substances is injected, each substance travels through the column at a different speed and takes a different amount of time (which is defined as the retention time, ι) to reach the end of column. The retention time depends on the solubility of the sample I the column liquid.

GC is used to determine the reference quantity of ethanol in fermenting grape juice in this research. In this method, an internal standard (propanol) is used to compensate for differences that may arise because of the nature of the sample and standards, and the way in which the sample is introduces in to the GC. By adding the same amount of internal standard to the standards and sample, it can be used as a constant reference, and the ratio of the analytical response can be taken due to analyte (ethanol) to the response of the internal standard (propanol), to correct for any mishandling.

B.2 Determination of Wine Ethanol Content

B.2.1 Identification of the Ethanol Retention Time

Firstly, fill a 1 μl syringe with 0.1 μl of the mixed alcohols. Then inject the sample into the GC as per demonstrator's instructions. Wait for the peaks to appear and record the times of each peak, which is the retention time. Finally, repeat using samples of the individual alcohols.

B.2.2 Quantification of Ethanol in Fermenting Grape Juice

Take 5 clean 25ml volumetric flasks and use the autopipettes to make up the following solutions with distilled water to the volumetric flask mark after adding the alcohol.

Table B-1 Standard and sample solutions for GC ethanol determination.

Solution	Ethanol	Propanol	Ethanol Con.
Standard 1	100 μl	500 μl	0.4 %v/v
Standard 2	100 μl	500 μl	0.8 %v/v
Standard 3	100 μl	500 μl	1.2 %v/v
Standard 4	100 μl	500 μl	1.6 %v/v
Grape Juice Sample	2ml sample	500 μl	?

Run the sample and standards on the GC and record the peak area for ethanol and propanol. Plot the ethanol peak area/propanol peak area on the vertical axis, and volume of ethanol/volume of propanol on the horizontal axis of a calibration curve. Read off the value of volume of ethanol/volume of propanol for your wine sample. The ethanol concentration in the wine sample can be calculated by following equation.

$$C_E\% = \frac{\text{Volume of ethanol}}{\text{Volume of propanol}} \times \frac{\text{Volume of propanol } (500\mu l)}{\text{total volume (25ml)}} \times 100 \qquad \text{(B-1)}$$

Appendix C
Publication List

[1] X. Liu, Q. J. Fang, I. Cosic, and S. Zheng, "Electrical Impedance Spectroscopy Investigation on Banana Ripening," in *Proceedings of the Europe - Asia Symposium on Quality Management in Postharvest Systems*, pp. 159-165, Bangkok, Thailand, 2007.

[2] X. Liu, Q. J. Fang, I. Cosic, S. Zheng, and P. Cao, "Electrical Impedance Spectroscopy Investigation on Cucumber Dehydration," in *Proceedings of the Europe - Asia Symposium on Quality Management in Postharvest Systems*, pp. 637-644, Bangkok, Thailand, 2007.

[3] S. Zheng, Q. J. Fang, and I. Cosic, "An Investigation on Dielectric Properties of Major Constituents of Grape Must Using Electrochemical Impedance Spectroscopy," *European Food Research and Technology*, 2009. In press. DOI 10.1007/s00217-009-1126-9; Available online: http://www.springerlink.com/openurl.asp?genre=article&id=doi:10.1007/s00217-009-1126-9

Note: Full papers are attached in the enclose CD.

Appendix D
Raw Data and Statistics Data

The raw data and statistics data of all the experiments on pure solutions, compound solutions and validation tests, are attached in the enclosed CD.